Salmonella actively modulates TFEB in murine macrophages in a growth-phase and time-dependent manner

Subothan Inpanathan*[1,2], Erika Ospina-Escobar*[1,2], Vanessa Cruz Li[1], Zainab Adamji[1,2], Tracy Lackraj[1], Youn Hee Cho[1,2], Natasha Porco[1,2], Christopher H. Choy[1,2], Joseph B. McPhee[1,2], and Roberto J. Botelho[1,2,#]

[1]Department of Chemistry and Biology and [2]Molecular Science Graduate Program, Toronto Metropolitan University, Toronto, Ontario, Canada, M5B2K3

*Equal contribution

#To whom correspondence should be sent to: Dr. Roberto Botelho, Dept. of Chemistry and Biology, Toronto Metropolitan University, Toronto, ON, Canada, M5B2K3; E-mail: rbotelho@ryerson.ca

Keywords

Bacteria, macrophages, transcription factors, cell adaptation, innate immunity, *Salmonella*, culture, lysosomes

Running title: *Salmonella* and TFEB in macrophages

Summary

The transcription factor TFEB drives expression of lysosomal, autophagic, and immune-responsive genes in response to LPS and phagocytosis. Interestingly, compounds that promote TFEB activity enhance bactericidal activity while intracellular pathogens like *Mycobacterium* and *Salmonella* repress TFEB. However, *Salmonella enterica* sv. Typhimurium (*S.* Typhimurium) was reported to actively stimulate TFEB, implying a benefit to *Salmonella*. To better understand the relationship between *S.* Typhimurium and TFEB, we assessed if *S.* Typhimurium regulated TFEB in macrophages in a manner dependent on infection conditions. We observed that macrophages that engulfed late-logarithmic grown *Salmonella* accumulated nuclear TFEB, comparable to macrophages that engulfed *E. coli*. In contrast, stationary-phase *S.* Typhimurium infection of macrophages actively delayed TFEB nuclear mobilization. The delay in TFEB nuclear mobilization was not observed in macrophages that engulfed heat-killed stationary-phase *Salmonella*, or *Salmonella* lacking functional SPI-1 and SPI-2 type three secretion systems. *S.* Typhimurium mutated in the master virulence regulator *phoP* or the secreted effector genes *sifA*, and *sopD* also showed TFEB nuclear translocation. Interestingly, while *E. coli* survived better in *tfeb*$^{-/-}$ macrophages, *S.* Typhimurium growth was similar in wild-type and *tfeb*$^{-/-}$ macrophages. Moreover, *Salmonella* survival was not readily affected by its growth phase in wild-type or knockout macrophages, though in HeLa cells late-log *Salmonella* benefitted from the loss of TFEB. Priming macrophages with phagocytosis enhanced the killing of *Salmonella* in wild-type, but not in *tfeb*$^{-/-}$ macrophages. Collectively, *S.* Typhimurium orchestrate TFEB in a manner dependent on infection conditions, while disturbing this context-dependent control of TFEB may be detrimental to *Salmonella* survival.

Importance

Activation of the host transcription factor TFEB helps mammalian cells adapt to stresses such as starvation and infection by upregulating lysosome, autophagy, and immuno-protective gene expression. Thus, TFEB is generally thought to protect host cells. However, it may also be that pathogenic bacteria like *Salmonella* orchestrate TFEB in a spatio-temporal manner to harness its functions to grow intracellularly. Indeed, the relationship between *Salmonella* and TFEB is controversial since some studies showed that *Salmonella* actively promotes TFEB, while others have observed that *Salmonella* degrades TFEB and that compounds that promote TFEB restrict bacterial growth. Our work provides a path to resolve these apparent discordant observations since we showed that stationary-grown *Salmonella* actively delays TFEB after infection, while late-log *Salmonella* is permissive of TFEB activation. Nevertheless, the exact function of this manipulation remains unclear, but conditions that erase the conditional control of TFEB by *Salmonella* may be detrimental to the microbe.

Introduction

Macrophages are innate immune cells that hunt and engulf microbes through phagocytosis. As a corollary, following phagocytosis, microbes are quarantined within phagosomes, which are then transformed into hostile phagolysosomes. During this maturation process, phagosomes acquire a microbicidal milieu enriched in hydrolytic enzymes, antimicrobial peptides, and an acidic and oxidative lumen (Flannagan *et al.*, 2012; Levin *et al.*, 2016; Nguyen and Yates, 2021; Fountain *et al.*, 2021).

Phagosome maturation is critically dependent on the endolysosomal membrane system. Phagosomes fuse sequentially with endosomes and ultimately with lysosomes in a process that depends on various Rab GTPases, lipid mediators like phosphatidylinositol-3-phosphate, and motor and SNARE proteins (Bouvier *et al.*, 1994; Fratti *et al.*, 2001:7; Harrison *et al.*, 2003; Vieira *et al.*, 2003; Pei *et al.*, 2014; Kim *et al.*, 2014; Levin *et al.*, 2016; Nguyen and Yates, 2021; Fountain *et al.*, 2021; Fountain *et al.*, 2021). Interestingly, while phagosome-lysosome fusion has been known for decades (Brandes and Anton, 1969; Kielian and Cohn, 1980), it was generally assumed that lysosomes and their properties remained unchanged during phagocytosis, phagosome maturation, and interaction with microbes – though at least one study in 1970s suggested that phagocytosis in macrophages induced lysosomal enzyme levels (Axline and Cohn, 1970). However, we now understand that lysosomes are remodelled in response to various stresses, including interaction with microbes, microbe-associated molecular patterns (MAMPs), and phagocytosis (Swanson *et al.*, 1987; Vyas *et al.*, 2007; Mrakovic *et al.*, 2012; Pastore *et al.*, 2016; Gray *et al.*, 2016; Brady *et al.*, 2018; Hipolito *et al.*, 2018; Sachdeva *et al.*, 2020; Najibi *et al.*, 2022). In part, this is achieved by activation of the transcription factor TFEB, which drives expression of endolysosomal, autophagy, and immunomodulatory genes (Settembre *et al.*, 2011; Visvikis *et al.*, 2014; Pastore *et al.*, 2016; Gray *et al.*, 2016; Brady *et al.*, 2018; Hipolito *et al.*, 2018).

TFEB is activated by numerous signals including amino acid deprivation, metabolic stress, mitochondrial stress, lipid metabolism and several immune stimuli such as phagocytosis of IgG-coated particles, several types of bacteria, and pattern recognition receptors that bind MAMPs (Settembre *et al.*, 2011; Settembre *et al.*, 2012; Roczniak-Ferguson *et al.*, 2012; Tsunemi *et al.*, 2012; Settembre *et al.*, 2013a; Settembre *et al.*, 2013b; Visvikis *et al.*, 2014; Nezich *et al.*, 2015;

Najibi *et al.*, 2016; Pastore *et al.*, 2016; Gray *et al.*, 2016; Inpanathan and Botelho, 2019; Hipolito *et al.*, 2019). TFEB activation increases intracellular killing of microbes like *Escherichia coli*, *Mycobacterium tuberculosis*, *S.* Typhimurium, *Staphylococcus aureus* and *C. albicans*. (Gray *et al.*, 2016; Rao *et al.*, 2020; Ammanathan *et al.*, 2020; Westman *et al.*, 2020). Overall, TFEB activation is thought to favour immune function and repress microbe survival (Brady *et al.*, 2018; Hipolito *et al.*, 2018; Irazoqui, 2020). However, there is evidence for some microbes actively manipulating TFEB function.

Macrophages that engulfed living *S.* Typhimurium displayed nuclear TFEB translocation relative to macrophages that internalized non-viable *S.* Typhimurium in a process dependent on PLC-PKD pathway (Najibi *et al.*, 2016). A more recent study by the same authors indicate that dead *Salmonella* can also activate TFEB, but more slowly (Najibi *et al.*, 2022). Nevertheless, the intentional stimulation of TFEB by invading microbes is peculiar since TFEB stimulation is typically thought to benefit the host. Indeed, additional studies suggest that ectopic activation of TFEB with compounds like VX-765, acacetin and 4-octyl itaconate can limit *Salmonella* survival (Rao *et al.*, 2020; Ammanathan *et al.*, 2020; Zhang *et al.*, 2022). Collectively, these observations suggest a complex interplay between TFEB and *S.* Typhimurium that requires further investigation.

S. Typhimurium is a microbe that hijacks mammalian cells through a complex virulence program involving two type III secretion systems (T3SS), SPI-1 and SPI-2, that collectively inject ~50 bacterial effector proteins into infected host cells that manipulate the behaviour of both epithelial and immune cells (Portaliou *et al.*, 2016; Jennings *et al.*, 2017; Lou *et al.*, 2019). The SPI-I T3SS is usually associated with invasion of epithelial cells, a bacteria-driven process that remodels the epithelial cell plasma membrane to ruffle and internalize the bacteria (Lundberg *et*

al., 1999; Terebiznik *et al.*, 2002; Raffatellu *et al.*, 2005; Patel and Galán, 2005; Bruno *et al.*, 2009; Lou *et al.*, 2019). *S.* Typhimurium can also infect macrophages during macrophage-driven phagocytosis (Cirillo *et al.*, 1998; Drecktrah *et al.*, 2006). Here, *S.* Typhimurium does not have to be in an invasive state *per se*, but the SPI-2 T3SS is essential to usurp, remodel and even escape the *Salmonella*-containing vacuole to promote its replication within the host macrophage (Cirillo *et al.*, 1998; Shea *et al.*, 1999; Drecktrah *et al.*, 2006; Jennings *et al.*, 2017). Importantly, the behaviour of *Salmonella* within a host cell may depend on both bacterial and host cell conditions including entry mode, growth and metabolic state, and time post-infection (Deiwick *et al.*, 1999; Lundberg *et al.*, 1999; Drecktrah *et al.*, 2006; Ibarra *et al.*, 2010; Lathrop *et al.*, 2015; Kurtz *et al.*, 2020). In fact, the growth state and nutritional conditions of *Salmonella* appear to modulate the entry mode, where late-log/early stationary phase grown *Salmonella* favour SPI-1 expression, while late stationary growth primes SPI-2 expression (Song *et al.*, 2004; Bustamante *et al.*, 2008; Ibarra *et al.*, 2010).

Given this, we postulated that *Salmonella* and TFEB activation may depend on the invasive state of *Salmonella* and/or bacterial growth conditions. Here, we provide evidence that *Salmonella* grown to stationary-phase actively and transiently represses TFEB in macrophages. In comparison, *Salmonella* grown to late log-phase promotes early translocation of TFEB to the nucleus. Moreover, while TFEB is needed to suppress *E. coli* survival in macrophages, its deletion had no apparent effect on *Salmonella* growth in macrophages. Yet, pre-activation of TFEB by phagocytosis increased killing of both bacterial species. Overall, we reveal a complex interplay between TFEB and *Salmonella* infection conditions.

Results

Salmonella grown to stationary phase delays activation of TFEB after uptake by macrophages

Phagocytosis of IgG-coated particles, unopsonized *E. coli*, *M. smegmatitis, and S. aureus*, and invasive *Salmonella* all activate TFEB in macrophages (Visvikis *et al.*, 2014; Najibi *et al.*, 2016; Pastore *et al.*, 2016; Gray *et al.*, 2016; Najibi *et al.*, 2022). In most cases, TFEB activation is thought to boost the immunological response by stimulating lysosomal, autophagy and immune-protective genes (Visvikis *et al.*, 2014; Pastore *et al.*, 2016; Gray *et al.*, 2016; Brady *et al.*, 2018). However, in the case of invasive *Salmonella*, activation of TFEB has been reported to be driven by *Salmonella*, which implies a benefit to the microbe during invasion of macrophages (Najibi *et al.*, 2016). In apparent conflict with these observations, there are also observations showing that *Salmonella* represses TFEB and that TFEB stimulation increases *Salmonella* killing (Rao *et al.*, 2020; Ammanathan *et al.*, 2020). Given these discrepancies, we sought to better understand the relationship between *Salmonella* infection and TFEB activation.

We began by comparing the ability of *Salmonella* grown to stationary phase to elicit TFEB activation in macrophages by measuring the relative nuclear to cytosolic (N/C) ratio of TFEB. Stationary-phase *Salmonella* cultures are reported to be enriched in non-invasive *Salmonella*, and like *E. coli*, engulfment is thought to be driven by macrophage phagocytosis rather than by invasion (Drecktrah *et al.*, 2006; Gog *et al.*, 2012). As expected, we found that phagocytosis of non-pathogenic *E. coli* DH5α increased the N/C ratio of GFP-TFEB in RAW macrophages within 1 h of phagocytosis relative to resting macrophages (Fig. 1A, B). By contrast, the N/C ratio of GFP-TFEB in macrophages that engulfed stationary-phase *Salmonella* was similar to resting cells and significantly lower than macrophages that engulfed *E. coli* (Fig. 1A, B). Moreover, phagocytosis of heat-killed *Salmonella* previously grown to stationary-phase elicited nuclear mobilization of GFP-TFEB that was comparable to macrophages that engulfed *E. coli* (Fig. 1A,

B). Collectively, these observations suggest that stationary-phase *S.* Typhimurium actively represses TFEB nuclear translocation in macrophages at 1 h post-infection. However, we also observed an increase over time in the N/C ratio of GFP-TFEB in macrophages that engulfed stationary-phase *Salmonella*; at 4 and 6 h post-engulfment, the N/C ratio of GFP-TFEB in these cells was higher than resting cells or those at 1 h post-infection, and comparable to macrophages infected with *E. coli* (Fig. 1C, D). Thus, stationary-phase *Salmonella* delays TFEB mobilization to the nucleus, rather than fully arresting it.

Salmonella growth conditions affect TFEB response in macrophages

The growth phase of *Salmonella* is thought to affect the expression of invasion effectors and modulate the mode of infection (Lundberg *et al.*, 1999; Drecktrah *et al.*, 2006; Ibarra *et al.*, 2010). Typically, *Salmonella* is grown to late log-phase before experimentation. We thus tested whether the growth phase of *Salmonella* affected the N/C ratio of TFEB in RAW cells. First, we observed that stationary- and log-phase *E. coli* similarly induced nuclear translocation of TFEB (Fig. 2A, B). Moreover, TFEB remained enriched in its nuclear distribution in macrophages 1 h or 4 h post-uptake of *E. coli* grown to either culture phase (Fig. 2A, C, D). *Salmonella* infected cells displayed a contrasting behaviour in terms of TFEB nuclear entry. While stationary-phase *Salmonella* failed to activate TFEB at 1 h post-infection, as illustrated before, macrophages infected with late-logarithmic *Salmonella* significantly mobilized TFEB into the nucleus within 1 h of uptake (Fig. 2A, B), consistent with observations by Najibi *et al* (Najibi *et al.*, 2016). We observed similar results when staining for endogenously expressed TFEB; stationary-phase live *Salmonella* was the only condition that failed to enrich TFEB in the nucleus after 1 h of uptake, while live and dead *E.*

coli, live late log-phase *Salmonella*, and non-viable stationary-phase and late log-phase *Salmonella* all triggered accumulation of TFEB in the nucleus relative to resting cells (Fig. 3A-B).

We next tested if TFEB nuclear mobilization was subject to temporal modulation by *Salmonella* grown to either log- or stationary-phases by analysing the N/C ratio of TFEB at 1 or 4 h post-infection. As previously observed, macrophages infected with stationary-phase *Salmonella* displayed mostly cytosolic TFEB at 1 h post-infection and higher nuclear levels of TFEB at 4 h post-infection (Fig. 2A, C). In comparison, the N/C ratio of TFEB was similar between macrophages that engulfed log-phase *Salmonella* after 1 h or 4 h of infection, and both were statistically comparable to the counterpart macrophages that engulfed *E. coli* (Fig. 2A, 2D). Collectively, *Salmonella* modulates TFEB nuclear localization in macrophages in a manner dependent on its growth conditions and stage of infection. Specifically, *Salmonella* grown to stationary phase actively delays TFEB mobilization relative to *E. coli* or *Salmonella* grown to log-phase.

Salmonella growth conditions affect TFEB nuclear translocation in HeLa cells

Given our observations in RAW macrophages above, we next assessed if *Salmonella* grown to either stationary or late-log also caused differential nuclear translocation of endogenous TFEB in a non-macrophage cell model, for which we used HeLa cells. First, endogenous TFEB remained cytosolic in HeLa cells infected with *Salmonella* grown to either growth phase after 1 h (Fig. 4A, B). Yet, after 4 h post-infection we then observed an enrichment in nuclear TFEB relative to the cytosolic pool in HeLa cells infected with late-log *Salmonella*, but not in HeLa cells infected with stationary-grown *Salmonella* (Fig. 4A, B). The absence of nuclear TFEB in HeLa cells infected with stationary-grown Salmonella may reflect the less invasive nature of these bacteria, which

could affect uptake by non-phagocytes. However, TFEB remained predominantly cytosolic even in HeLa cells with larger number of engulfed *Salmonella*. Overall, we reveal that TFEB nuclear translocation in non-macrophage cells is also dependent on *Salmonella* growth conditions, and hence, context dependent.

The effect of Salmonella on TFEB phosphorylation

The cytosolic and nuclear distribution of TFEB can be regulated by the phosphorylation status at various residues of TFEB (Settembre *et al.*, 2012; Roczniak-Ferguson *et al.*, 2012:1; Martina *et al.*, 2012:1; Medina *et al.*, 2015; Puertollano *et al.*, 2018). To better understand how *Salmonella* might affect TFEB distribution in macrophages, we used Phos-tag gels to determine the general phosphorylation of TFEB using whole cell lysates (Nagy *et al.*, 2018) and quantified the band migration front of TFEB. To analyse total levels, we employed a standard SDS-PAGE gel and Western blotting.

As expected, cell lysates from macrophages that engulfed *E. coli* for 1 h displayed a TFEB band pattern that migrated faster relative to lysates from resting, *i.e.*, phagocytosis of *E. coli* caused a significant net dephosphorylation of TFEB (Fig. 5A, B). Interestingly, this was more variable in macrophages 4 h post-phagocytosis of *E. coli*. In comparison, infection with *Salmonella* for either 1 or 4 h appeared to have an intermediate and heterogeneous effect on TFEB phosphorylation (Fig. 5A, B). This result was not expected and may reflect a change in phosphorylation sites without a net change in number of phosphorylated residues of TFEB and/or heterogeneous infection rates that is not resolvable by a population-based assay such as Western blotting (Puertollano *et al.*, 2018), or may suggest that TFEB is regulated through another mechanism such as the recently discovered itaconate modification of TFEB (Zhang *et al.*, 2022; Schuster *et al.*, 2022).

Interestingly, the levels of total TFEB normalized to actin were reduced in macrophages infected for 4 h with late-log-phase *Salmonella*, indicating that under specific conditions, *Salmonella* can repress TFEB expression or promote its turnover (Fig. 5A, C, D), consistent with *Salmonella* infection of murine bone marrow-derived primary macrophages (Rao *et al.*, 2020). Overall, TFEB control by *Salmonella* is subject to a temporal sequence of events that include control of its levels and likely a complex pattern of post-translational modifications.

T3SS-1 and T3SS-2 secretion systems are needed for stationary phase-grown* Salmonella *to delay TFEB nuclear mobilization

Our data show that stationary-phase *Salmonella* actively delays TFEB mobilization into the nucleus after macrophage engulfment. To test whether SPI-1 and SPI-2 T3SS were involved in this delay, we permitted macrophages to engulf stationary-phase and log-phase *Salmonella* carrying loss-of-function mutations in *invA* and *ssaR genes*, which are respectively required to express subunits and/or form the SPI-1 and SPI-2 complexes (Collazo and Galán, 1997; Cirillo *et al.*, 1998; Hensel *et al.*, 1998; Lundberg *et al.*, 1999). As before, wild-type *Salmonella* grown to stationary phase did not elicit nuclear accumulation of TFEB, unlike *Salmonella* grown to log-phase (Fig. 6A, B). However, macrophages that engulfed *invA ssaR Salmonella* grown to either growth conditions displayed higher levels of nuclear TFEB relative to stationary-phase wild-type *Salmonella* (Fig. 6A, B). We note that single *invA* and *ssaR* mutants had intermediate effect on TFEB localization, suggesting some redundancy towards TFEB manipulation (not shown). Thus, *Salmonella* SPI-1/SPI-2 double mutants fail to repress TFEB activation during phagocytosis and we predict that TFEB activation is now a host-driven process. In conclusion, our data suggest that

live *Salmonella* grown to stationary phase actively represses TFEB in a time-dependent and effector-dependent manner.

TFEB repression depends on PhoP, SifA and SopD2

Stationary-phase *Salmonella* appear to actively delay TFEB nuclear migration during macrophage infection. To further determine if stationary-phase *Salmonella* actively repress TFEB, we examined TFEB nuclear mobilization in macrophages after engulfment of seven *Salmonella* mutants; these mutants were either disrupted in the master virulence regulator, PhoP (Δ*phoP*) or eliminated effectors of the *Salmonella* SPI-2 system known to alter intracellular signalling and membrane trafficking (Δ*sopD2*, Δ*sopA*, Δ*sifA*, Δ*pipB2*, Δ*sspH2*, Δ*slrP*, or Δ*sigD*); (Brumell *et al.*, 2003:2; Geddes *et al.*, 2005; Figueira *et al.*, 2013; Jennings *et al.*, 2017:2) These *Salmonella* mutants were grown to stationary phase since this is the bacterial growth condition that actively suppressed TFEB nuclear entry. Of these seven mutants, we identified three whose phagocytosis triggered significant activation of GFP-tagged and endogenous TFEB relative to wild-type *Salmonella*: *sopD2*, *sifA* and *phoP* (Fig. 7). These data further support a functional role for *Salmonella* in impeding early TFEB activation after phagocytosis by macrophages. We speculate that the PhoPQ two-component system is necessary to sense the intra-phagosomal environment of engulfed *Salmonella* eliciting expression of effectors that delay TFEB activation such as effectors of the SPI-II system (Deiwick *et al.*, 1999; Bijlsma and Groisman, 2005; Martin-Orozco *et al.*, 2006; Prost and Miller, 2008). In turn, SopD2 and SifA are known to alter intracellular signalling and trafficking, which may prevent activation of TFEB (Brumell *et al.*, 2003:2; Dumont *et al.*, 2010; McEwan *et al.*, 2015; D'Costa *et al.*, 2015:2). These observations support a model whereby stationary-grown *Salmonella* actively repress TFEB, at least in the early stages of infection.

Impact of Salmonella growth phase on gene expression in macrophages

To understand if the delay in TFEB nuclear entry by stationary-grown *Salmonella* reprogrammed lysosome and autophagy gene expression relative to infection with late-log *Salmonella*, we quantified by qRT-PCR the expression of the model genes, LC3, LAMP1, and cathepsin D. We used wild-type, *tfeb*$^{-/-}$, and *tfeb*$^{-/-}$ *tfe3*$^{-/-}$ RAW cells, previously described (Pastore *et al.*, 2016). First, deletion of TFEB and/or TFE3 did not significantly decrease basal expression of these genes (Fig. 8A). Second, the mRNA levels of LAMP1, cathepsin D, and LC3 all behaved distinctly depending on infection, time, and genotype. For example, neither genotype, infection mode, nor post-infection time significantly altered the levels of LAMP1 mRNA (Fig. 8B, C). In comparison, cathepsin D mRNA levels increased in wild-type RAW cells 20 h post-infection with either stationary or late-log *Salmonella* (Fig. 8D). However, it was unclear if this depended on TFEB/TFE3; while the increase in cathepsin D mRNA is eliminated in *tfeb*$^{-/-}$ macrophages after infection, the baseline appears higher in all conditions relative to wild-type macrophages (even if not statistically significant in Fig. 8A). Additionally, while stationary-grown *Salmonella* did not elicit a statistically significant increase in cathepsin D mRNA in *tfeb*$^{-/-}$ *tfe3*$^{-/-}$, unlike in wild-type macrophages, there was still an increase in cathepsin D mRNA in macrophages infected with late-log *Salmonella* (Fig. 8D). Moreover, we could not detect statistical differences when comparing the genotypes at 20 h post-infection (Fig. 8E). Lastly, LC3 mRNA levels did not change in wild-type macrophages infected with either growth phases of *Salmonella* (Fig. 8F). Yet, and surprisingly, *tfeb*$^{-/-}$ and *tfeb*$^{-/-}$ *tfe3*$^{-/-}$ macrophages displayed augmented LC3 mRNA expression levels infected with late-log *Salmonella* (Fig. 8F, G). Overall, stationary vs. late-log *Salmonella* may elicit distinct gene expression patterns in infected macrophages and some of these may depend

on TFEB/TFE3, but dissecting this may require more sophisticated approaches such as RNA-seq even single-cell transcriptomics given the variability the in number of bacteria per macrophage.

Stationary and late-log Salmonella differentially impact autophagy in macrophages

We also queried the state of autophagy and xenophagy, both of which can be affected by *Salmonella* and TFEB. To this end, we transfected wild-type, *tfeb*$^{-/-}$, and *tfeb*$^{-/-}$ *tfe3*$^{-/-}$ RAW cells with the mCherry-GFP-LC3 reporter. This chimeric protein reports on both the number of autophagosomes (mCherry puncta) and autophagosome maturation, which can be determined by the quenching of GFP fluorescence in the low pH of autolysosomes (N'Diaye *et al.*, 2009; Maejima *et al.*, 2013).

First, we observed minor differences in the number of autophagosomes (LC3-mCherry) between wild-type, *tfeb*$^{-/-}$, and *tfeb*$^{-/-}$ *tfe3*$^{-/-}$ RAW cells (Fig. 9A-D). Interestingly, wild-type RAW cells infected with late-log *Salmonella* generally had significantly fewer autophagosomes than macrophages infected with stationary-grown *Salmonella* (Fig. 9E). However, this difference between infection with stationary or late-log *Salmonella* remained when the host cells were mutated for TFEB and/or TFE3 (Fig. 9F, G). Moreover, we did not observe a significant difference in autophagosome maturation or xenophagy that depended on genotype of macrophages, bacterial growth phase, and time of infection (Fig. 10). Overall, again, while there may be differences on autophagy triggered by bacterial growth phase, our data does not indicate that these depend on TFEB manipulation, though it is possible than extending time of infection may lead to differences based on trends observed.

TFEB expression impacts E. coli and Salmonella survival differently in macrophages

Our observations indicate that TFEB distribution in macrophages during *Salmonella* uptake is dependent on *Salmonella* growth conditions, wherein stationary *Salmonella* transiently, but actively represses TFEB, while invasive *Salmonella* permits or elicits nuclear translocation of TFEB. In comparison, phagocytosis of non-pathogenic *E. coli* always triggers nuclear entry of TFEB in macrophages irrespective of the growth conditions of *E. coli* and over the observed period. This raises the question of whether TFEB helps repress *Salmonella* or enables *Salmonella* growth in macrophages.

To better understand this potential conundrum, we investigated the survival of stationary-grown *E. coli* and *Salmonella* within wild-type and *tfeb*$^{-/-}$ RAW macrophages (Pastore *et al.*, 2016). To do this, we allowed macrophages to phagocytose bacteria for 1 h, followed by gentamicin treatment to kill external bacteria. Macrophages were then lysed or chased for an additional 4 h to respectively assess bacterial uptake and survival within macrophages. Lysates were plated and the number of colonies formed were scored and normalized against the initial uptake. For *E. coli*, we observed a significant increase in bacterial survival in *tfeb*$^{-/-}$ RAW macrophages compared to wild-type RAW cells (Fig. 11A), consistent with previous results (Gray *et al.*, 2016). By contrast, we did not observe a difference in *Salmonella* survival infecting wild-type or *tfeb*$^{-/-}$ RAW macrophages (Fig. 11B). We then tested if the growth-phase of Salmonella affected survival in wild-type and in *tfeb*$^{-/-}$ *tfe3*$^{-/-}$ RAW cells (Pastore *et al.*, 2016). As before, we did not observe any significant differences in Salmonella survival at 4 h post-infection that dependent on TFEB/TFE3 and growth-phase of the bacteria (Fig. 11C). At 20 h post-infection, we also did not observe a statistically significant difference between these conditions, but we note the low p values, which might indicate a trend (Fig. 11C). Overall, our observations suggests that TFEB aids macrophages

in killing *E. coli*, but there is an equivocal effect on *Salmonella* survival, which may reflect a dual role of TFEB towards *Salmonella* that depends on its tight regulation by both host and microbe.

To complement our work in macrophages, we also investigated the importance of TFEB and related factors in intracellular survival of stationary and late-log grown *Salmonella* in HeLa cells. We used wild-type HeLa and HeLa cells triple-deleted for *tfeb*$^{-/-}$ *tfe3*$^{-/-}$ *mitf*$^{-/-}$ *(HeLa-TKO;* (Nezich *et al.*, 2015)*)* and measured *Salmonella* survival at 4 and 20 h post-infection. During the first 4 h post-infection, we did not observe a difference in *Salmonella* survival by either bacterial growth condition or host genotype (Fig. 11D). In contrast, we observed a significant difference in survival at 20 h post-infection; whereas stationary-grown *Salmonella* exhibited similar survival in wild-type and HeLa-TKO cells, late-log *Salmonella* coped better within HeLa-TKO cells relative to wild-type HeLa host cells (Fig. 11D). This indicates that TFEB-family proteins help neutralize *Salmonella* in non-macrophage cells.

Pre-activation of TFEB by previous IgG-phagocytosis boosts Salmonella killing in macrophages

Our work suggests that *Salmonella* may orchestrate a temporal sequence of TFEB repression and activation that suits the stage of infection within macrophages. We hypothesized that disrupting this timed sequence may be detrimental to *Salmonella*. To test this, we employed an initial round of phagocytosis of IgG-coated beads, which we previously showed activates TFEB and enhances degradation of lysosomes and killing of *E. coli* (Gray *et al.*, 2016). Specifically, Fcγ receptor-mediated phagocytosis activates TFEB by releasing Ca^{2+} from lysosomes during phagosome maturation, enhancing lysosomal gene expression (Gray *et al.*, 2016). Thus, we pre-treated wild-type and *tfeb*$^{-/-}$ RAW macrophages with vehicle or IgG-coated beads, followed by phagocytosis of

stationary phase *E. coli* or *Salmonella*, and then chased for 1 h to determine uptake or for 4 h to determine killing. The number of colonies formed was normalized to 1 h condition. As before, we observed increased *E. coli* survival in *tfeb*$^{-/-}$ macrophages relative to wild-type macrophages without priming (Fig. 12A; percent survival: 84% ± 5%, and 130% ± 11% in wild-type and in *tfeb*$^{-/-}$ macrophages, respectively). In comparison, *Salmonella* survived about the same in both genotypes (Fig. 12B; 160 ± 15% vs. 187% ± 19% in wild-type and in *tfeb*$^{-/-}$ macrophages, respectively). When wild-type macrophages were primed with IgG-coated beads, we observed reduced survival of 57% ± 9% for *E. coli*, compared to 84% in unprimed wild-type macrophages (Fig. 12A). This drop in survival was eliminated in *tfeb*$^{-/-}$ macrophages (Fig. 12A; 130%±11% vs. 137±`13%, unprimed vs. primed). Interestingly, priming wild-type macrophages abated *Salmonella* survival (Fig. 12B; 94%±11% vs. 160±15%, primed vs. unprimed), which was lost in *tfeb*$^{-/-}$ macrophages (Fig. 12B; 187% ± 19% vs. 196% ± 26%, unprimed vs. primed).

To complement these observations, we extended pre-activation of TFEB using apilimod, an inhibitor of PIKfyve that stimulates TFEB (Choy *et al.*, 2018). However, apilimod treatment had little effect in *Salmonella* survival in both wild-type and *tfeb*$^{-/-}$ macrophages under our experimental conditions, which may reflect a more complex relationship between TFEB activation and PIKfyve-mediated membrane trafficking (Fig. 12C). Collectively, our observations with IgG-primed phagocytosis suggests that pre- or forced activation of TFEB can restrict *Salmonella* survival in macrophages.

Discussion

Recent work has highlighted the role of TFEB as a conserved immunoprotective transcription factor that promotes lysosomal and autophagic activities, antimicrobial peptide production, and

modulation of cytokine secretion in response to various immune stimuli (Visvikis *et al.*, 2014; Pastore *et al.*, 2016; Gray *et al.*, 2016; Brady *et al.*, 2018; Najibi *et al.*, 2022). Previous research showed that *Salmonella* can actively stimulate TFEB in RAW macrophages (Najibi *et al.*, 2016; Najibi *et al.*, 2022), suggesting that TFEB activation provides an advantage to this microbe. However, this model appears inconsistent with observations that i) *Salmonella* represses TFEB to escape macrophage clearance and ii) acacetin-induced activation of TFEB in HeLa cells enhances killing of *Salmonella* by stimulating xenophagy (Rao *et al.*, 2020; Ammanathan *et al.*, 2020). Collectively, this implies that the relationship between *Salmonella* and TFEB is multi-layered and possibly dependent on infection conditions. Indeed, our observations support this view since the effect on *Salmonella* on TFEB was affected by the bacterial growth conditions and time of infection, whereby stationary, but not late-log bacteria, delayed TFEB activation. Furthermore, inactivation of the SPI-1 and SPI-2 T3SS of *S.* Typhimurium abrogated the inhibition of TFEB-nuclear translocation. The same effect was also seen when the master regulator, *phoP*, or the secreted effectors *sopD2* or *sifA* were deleted. Moreover, while deleting TFEB in macrophages protected *E. coli* from phagocytic killing, there was no effect on *Salmonella* survival. In comparison, promoting TFEB before infection enhanced killing of both bacterial species.

Host cell-dependent upregulation of TFEB

TFEB is subject to a complex regulatory network involving phosphorylation and other post-translational modifications (Bao *et al.*, 2016; Puertollano *et al.*, 2018; Zhang *et al.*, 2022). In the context of phagocytosis, host cells engage a signalling axis that promotes reactive oxygen species, which activates CD38 and synthesis of the second messenger NAADP (Najibi *et al.*, 2022). This in turn seems to activate MCOLN1/TRPML1 to release intraphagosomal Ca^{2+} to stimulate

calcineurin, which then dephosphorylates and promotes TFEB nuclear entry (Gray *et al.*, 2016; Najibi *et al.*, 2022). This process is clearly driven by the host cell in response to microbe engulfment and phagocytosis (Gray *et al.*, 2016; Najibi *et al.*, 2022). Additionally, host macrophages engage a TFEB-Irg1-itaconate signalling axis in response to *Salmonella*, whereby TFEB promotes Irg1-driven itaconate production. Itaconate then alkylates and promotes TFEB nuclear translocation, which helps restrict *Salmonella* survival (Zhang *et al.*, 2022; Schuster *et al.*, 2022). As described, the activation of TFEB is macrophage-driven. We propose that stationary *Salmonella* actively delays macrophage-driven TFEB stimulation because living stationary *Salmonella* repressed TFEB nuclear translocation, while non-viable stationary *Salmonella* or mutants in *invA ssrA*, *phoP*, *sifA*, and *sopD2* did not. We do not know how stationary *Salmonella* delays TFEB activation, but we propose here that virulence factors like SopD2 may prevent NAADP-Ca^{2+} signalling or block itaconate action. In fact, *Salmonella*, as well as *Yersinia pestis* can degrade itaconate to enhance their survival in macrophages since itaconate compromises the glycoxylate cycle whereby bacteria can use host cell resources for energy production (Sasikaran *et al.*, 2014; Hersch and Navarre, 2020). Lastly, similar mechanisms may be at play during infection of non-macrophages since stationary *Salmonella* did not elicit TFEB nuclear entry in HeLa cells, while infection with late-log *Salmonella* did after 4 h.

Salmonella-dependent upregulation of TFEB

Viable *Salmonella* was observed to more readily promote TFEB compared to non-viable *Salmonella* by engaging a conserved PC-PLC-PKD pathway (Najibi *et al.*, 2016; Najibi *et al.*, 2022). This contrasts with observations that *Salmonella* represses and reduces TFEB levels (Rao *et al.*, 2020). In our hands, while stationary *Salmonella* actively delays TFEB nuclear translocation,

we did observe that late logarithmic-phase *Salmonella* triggers TFEB early during infection, which is consistent with Najibi *et al.* (Najibi *et al.*, 2016). However, contrary to their observations, dead *Salmonella* still activated TFEB in RAW macrophages – we do not know the reason for this discrepancy. It is also not unknown if any benefit exists for late-log *Salmonella* to promote or permit TFEB engagement; for example, it may be that specific temporal activation of TFEB may aid *Salmonella* in remodelling phagosomes or *Salmonella*-containing vacuoles. Perhaps aligning with the idea that the stage of infection is critical for what TFEB might do, we observed that late-log *Salmonella* reduced TFEB levels after 4 h of infection, consistent with reduced TFEB expression and lysosomal activity observed by Rao *et al.* (Rao *et al.*, 2020).

Mechanistic control of TFEB by Salmonella

How might stationary-phase *Salmonella* delay TFEB activation? Control of the expression of the SPI-1 and SPI-2 T3SS and their effectors depends on numerous regulatory inputs, including the phase of *Salmonella* growth (Portaliou *et al.*, 2016; Jennings *et al.*, 2017; Lou *et al.*, 2019). Specifically, late logarithmic phase growth promotes expression of SPI-1 and epithelial cell invasion, while stationary phase-growth promotes SPI-2 expression (Song *et al.*, 2004; Bustamante *et al.*, 2008; Ibarra *et al.*, 2010). We note that single mutants SPI-1 (*invA*) and SPI-2 (*ssaR*) had intermediate effects on TFEB nuclear entry relative to wild-type and *invA ssaR* strains (not shown) – this may represent redundancy between T3SSs relative to TFEB modulation or adaptation of the single mutant bacteria by upregulating other T3SSs. On the other hand, *invA ssaR* double mutants grown to stationary phase failed to delay TFEB nuclear translocation, suggesting that *Salmonella* effectors are required for this. Given that *phoP*, *sifA*, and *sopD2* mutants also failed to delay TFEB nuclear translocation, this suggests that the PhoPQ two-component system and alteration of

membrane and intracellular signalling are involved in delaying TFEB nuclear entry. SopD2 is proposed to be a GTPase activating protein for the Rab7 GTPase, while SifA interacts with motor proteins to sculpt *Salmonella*-containing vacuoles into *Salmonella*-induced filaments (Brumell *et al.*, 2003:2; Dumont *et al.*, 2010; D'Costa *et al.*, 2015).

We do not know how these factors interfere with TFEB, but we propose several non-mutually exclusive possibilities. First, BioID analysis of SopD2 and SifA identifies LAMTOR subunits as potential interactors (D'Costa *et al.*, 2019), which may allow *Salmonella* to modulate mTORC1, responsible for phosphorylation and repression of TFEB. While we did not see a significant change in TFEB phosphorylation by Phos-tag gels in *Salmonella*-infected cells, this could reflect a different phosphorylation pattern without a change in net phosphate number. Second, stationary *Salmonella* may blunt reactive oxygen species (ROS), thus preventing NAADP-Ca^{2+} activation of TFEB after phagocytosis in macrophages (Najibi *et al.*, 2022). In fact, *Salmonella* appears to manipulate ROS in host cells (van der Heijden *et al.*, 2015; Kim *et al.*, 2022), though it is not clear if this depends on growth phase and time of infection. Third, as indicated above, stationary *Salmonella* may blunt itaconate action, thus reducing TFEB activation (Sasikaran *et al.*, 2014; Hersch and Navarre, 2020; Zhang *et al.*, 2022; Schuster *et al.*, 2022).

Functional outcomes of Salmonella growth phase and TFEB regulation

Here, we reveal that infecting with stationary or late-log grown *Salmonella* has distinct effects on host cells. First, TFEB nuclear activation was delayed or repressed in macrophages and HeLa cells infected with stationary grown *Salmonella*, but not with late-log *Salmonella*. Second, late-log *Salmonella* increased the levels of LC3 mRNA in TFEB and TFEB/TFE3-deleted macrophages relative to stationary-grown *Salmonella*. Third, and despite the second point above, late-log

Salmonella reduced the number of LC3-positive autophagosomes relative to stationary-grown *Salmonella* in macrophages. However, changes in LC3 and cathepsin D mRNA and the number of autophagosomes cannot readily be assigned to TFEB modulation by the growth phase of the bacteria. Part of the challenge may be the heterogeneity among single *Salmonella* cells in a given population, how many bacteria infect a macrophage, and the time of infection. Resolving the role of TFEB delay by stationary-grown *Salmonella* may thus require single-cell RNA-seq analyses or single-cell, time-resolved assays of gene expression. Nevertheless, there is clearly a difference in host outcomes when infecting with stationary vs. late-log *Salmonella*.

This may have implications for in vivo infection as well since exponential phase *Salmonella* are more readily cleared and killed by phagocytes in blood compared to stationary phase *Salmonella* (Benjamin *et al.*, 1986). Stationary phase *Salmonella* also resulted in reduced colonization in livers and spleen and prevented animal death by 12-18 hours compared to exponential phase bacteria suggesting greater virulence of exponential phase *Salmonella* as well as a greater ability to replicate *in vivo* (Benjamin *et al.*, 1986). Interestingly, another study showed the transition of *Salmonella* from exponential to stationary phase can induce rapid and extensive apoptosis of infected macrophages but not epithelial cells; a process dependent on the invA gene, required for functional T3SS, and hilA gene, a regulator of SPI-1 gene expression (Lundberg *et al.*, 1999). While these differences among stationary and late-log *Salmonella* may reflect alterations to the bacteria themselves, such as LPS remodelling (Benjamin *et al.*, 1986; Bravo *et al.*, 2008), modulation of host factors like TFEB may be important. Supporting this, we did observe an improved survivability of late-log *Salmonella* in HeLa cells deleted for TFEB and related factors relative to wild-type HeLa cells and to stationary *Salmonella*.

Ectopic activation of TFEB enhances bacterial killing in macrophages

TFEB plays a protective role against intracellular bacteria (Visvikis *et al.*, 2014; Gray *et al.*, 2016; Irazoqui, 2020; Zhang *et al.*, 2022; Schuster *et al.*, 2022). In fact, we previously showed that pre-activation of TFEB by stimulating Fcγ receptors with aggregated IgG, enhanced *E. coli* killing in macrophages (Gray *et al.*, 2016). In this context, TFEB activation required phagosome-lysosome fusion and the release of lysosomal Ca^{2+} via TRPML1 (Gray *et al.*, 2016). More recently, pre-activation of TFEB by acacetin also promoted killing of *Salmonella* and *S. aureus* (Rao *et al.*, 2020; Ammanathan *et al.*, 2020). This suggests that strategies that obligately activate TFEB, thus bypassing any spatiotemporal manipulation of TFEB by *Salmonella*, may be detrimental to this microbe. Indeed, we observed that phagocytosis of IgG-coated beads, which stimulates TFEB, enhanced killing of both *E. coli* and *Salmonella* in wild-type but not in *tfeb*$^{-/-}$ RAW macrophages. Thus, while it may be that *Salmonella* benefits from TFEB activation under specific conditions, treatments that erode control of *Salmonella* on TFEB appear detrimental to the microbe.

Overall, our work sheds additional light into the interactions between *Salmonella* and TFEB in host macrophages. Depending on bacterial growth conditions and stage of infection, we find that *Salmonella* can either delay TFEB activation, or permit, or even elicit TFEB activation. This raises the possibility that TFEB presents a double-edged sword for *Salmonella* – depending on infection stages, TFEB may be detrimental or beneficial to *Salmonella*. Importantly, forcibly promoting TFEB can override the spatio-temporal control of TFEB imposed by *Salmonella*, enhancing the killing capacity of macrophages. Thus, therapeutics that promote TFEB and related proteins may be useful to enhance killing of intracellular pathogens

Materials and Methods

Cell Culture, Plasmids and Transfection

The RAW 264.7 macrophage-like male murine cell line and the HeLa female human cell line were grown in Dulbecco's modified Eagle's medium (DMEM) supplemented with 10% (v/v) heat-inactivated fetal bovine serum (FBS) (Wisent, QC) at 37 °C and 5% CO_2 up to passage 20. Before plating, cells were washed with sterile phosphate-buffered saline (PBS, Wisent) and released by scraping in 5 mL of DMEM media. Cells were seeded into 6-well or 12-well plates at a confluency of 40% and used the following day. Using the same growth conditions, we also used RAW 264.7 cells that were deleted for *TFEB* gene (RAW *tfeb*$^{-/-}$ cells) or double-deleted for *TFEB* and *TFE3* genes (RAW *tfeb*$^{-/-}$ *tfe3*$^{-/-}$ cells) using CRISPR-Cas9. As control cells, we used RAW cells subject to non-targeting CRISPR-Cas9 process (wild-type RAW cells). These cell lines were obtained from Dr. Rosa Puertollano (National Institutes of Health, MD and were previously described (Pastore *et al.*, 2016). We also used HeLa cells deleted by CRISPR-Cas9 for TFEB, TFE3, and MITF (HeLa TKO), obtained as a kind gift from Dr. Richard Youle and previously characterized (Nezich *et al.*, 2015).

To express GFP-TFEB fusion protein, we used a plasmid provided by Dr. Shawn Ferguson (Yale University School of Medicine, CT) and previously described (Roczniak-Ferguson *et al.*, 2012). A plasmid #22418 encoding mCherry-GFP-LC3 was obtained from Addgene, originally provided by Jayantha Debnath and previously defined (N'Diaye *et al.*, 2009; Maejima *et al.*, 2013). RAW cells were seeded at a 20-30% confluency in a 12-well plate the day before, and then transfected with the plasmid encoding GFP-TFEB or mCherry-GFP-LC3 using FuGene HD transfection reagent (Promega, WI), following manufacturer's instructions. The transfection mix

was left on cells for 5 h followed by removal and addition of new media. Cells were used the following day.

Bacterial Strains and Culture

In this study, we used *Escherichia coli* DH5α, wild-type *Salmonella enterica sv.* Typhimurium (SL1344), and *S.* Typhimurium strain deleted for the *phoP* gene (Δ*phoP)* (Mulder *et al.*, 2012). *S. typhimurium* mutants (Δ*sopD2*, Δ*sifA*, Δ*slrp*, Δ*sigD (*Δ*sopB*), Δ*sspH2*, Δ*sopA*, Δ*pipB2*) were obtained from Dr. John H. Brumell at the Hospital for Sick Children (Toronto, ON). All bacterial strains were grown overnight in lysogeny broth (LB) at 37°C with shaking. To use stationary cultures, bacteria were pelleted, washed once with PBS, and resuspended in DMEM at OD600 ~0.8 and immediately used for infection. To prepare log-phase growth bacteria, an overnight culture was sub-cultured in the morning at 1:10 in fresh LB and then grown at 37°C for 3.5 h until reaching late-logarithmic phase (OD_{600} ~ 0.8), before pelleting, washing in PBS and resuspending in DMEM at OD_{600} ~0.8.

Phagocytosis and Infection Assays

For phagocytosis/invasion assays, RAW macrophages plated at 1-2x10^6 cells/well were exposed to either stationary-phase or late log-phase bacteria at a 100:1 multiplicity of infection (MOI). Phagocytosis was synchronized through centrifugation of the culture plates at 500 xg for 5 min at room temperature. Macrophages were allowed to phagocytose for 1, 4, or 6 h, unless stated otherwise. Depending on the application, cells were then subject to 50 µg/mL gentamicin to kill extracellular bacteria for 30 min, followed by either lysis with Laemmli buffer for Western blot

analysis or fixation with 4 % (v/v) paraformaldehyde (PFA) in PBS for 20 min and processing for imaging as described below. Similar approach was done for HeLa cell infections.

Bacterial Survival Assays

Prior to engulfment of unopsonized *E. coli* or *S.* Typhimurium, RAW macrophages remained untreated or were pre-activated with IgG-opsonized beads for 1 h, followed by a 3 h chase. Treated or untreated macrophages were then infected with stationary-phase bacteria (*E. coli* and *S.* typhimurium) at a final $OD_{600} = 1.0$. Uptake was synchronized through centrifugation at 400 *g* for 5 min. At 1 h post-infection, macrophages were washed 3x with PBS and replaced with DMEM media containing 50 µg/ml gentamicin to kill extracellular bacteria for 30 min. After, cells were washed 3x with PBS and either lysed immediately (uptake) with 200 µL 1% Triton X-100 for 5 min or the media was replaced with new DMEM supplemented with 10% FBS, containing low concentration of gentamicin (12 µg/ml), and incubated for 3 h at 37°C to allow time for phagosome maturation and bacteria killing. Prior to lysing, cells were washed multiple times with PBS and replaced with DMEM media containing 50 µg/ml gentamicin to kill extracellular bacteria for 30 min. They were then washed 3x with PBS and lysed with 200 µL 1% triton X-100 for 5 min and scraped to release bacteria. Cell lysates were re-suspended in 800 µL PBS and subjected to serial dilutions in LB broth, followed by plating of 10 µL in LB plates, and incubated overnight at 37 ºC. Colony numbers were counted and recorded to determine CFU/mL relative to uptake.

For *Salmonella* survival in wild-type and mutant RAW and HeLa cells, the above was done with some changes. Cells were plated in 12-well plates and used at a density of $1x10^6$ cells/well and infected with *S.* Typhimurium grown to stationary or late-logarithmic phase at an MOI of

100:1. Cells were lysed immediately after 1 h of phagocytosis followed by 30 min incubation in DMEM with 50 µg/ml gentamicin to estimate bacterial uptake or lysed at 4 or 20 h post-infection to estimate killing. Lysates were then resuspended in 500 µL of PBS, serially diluted and 10 µL were plated on LB plates, and these were incubated overnight. Colony numbers were counted and used to determine bacterial survival relative to uptake.

For pre-activation of TFEB by apilimod, macrophages were treated with vehicle or 20 nM apilimod (Toronto Research Chemicals, Toronto, ON) for 1 h, followed by bacterial infection with the drugs present. Cells were then lysed immediately to determine uptake of bacteria or chased for 4 h post-infection with the drug to determine survival.

Immunofluorescence and Fluorescence Microscopy

To visualize external bacteria in TFEB-GFP transfected cells, immunostaining was conducted by briefly washing cells 3x with 0.5% Bovine Serum Albumin (BSA) and then incubating cells for 30 min with either rabbit anti-*E. coli* antibodies (BioRad, ON) or rabbit anti-*Salmonella* O antiserum group B antibodies (Fisher Scientific, ON) at 1:500. Cells were then washed 3x with 0.5% BSA in PBS, followed by secondary donkey anti-rabbit antibodies conjugated to Dylight355 (Bethyl Laboratories, TX) for 30 min at 1:500 in 0.5% BSA in PBS. To visualize internal bacteria, cells were permeabilized with 1% triton X-100 in PBS, followed by incubation with the same primary antibodies above, but followed with donkey anti-rabbit antibodies conjugated to Dylight 550 (Bethyl Laboratories, TX). Cells were washed 3x with 0.5% BSA and mounted onto glass slides with fluorescent mounting media (DAKO) for imaging.

To stain for endogenous TFEB, cells were fixed with 4 % PFA (v/v) at room temperature for 20 min and 0.1 M glycine in PBS for 10 min, before being washed 3x with 0.5% BSA and

permeabilized with 0.1% triton for 10 min or using ice cold methanol for 5 min. Cells were blocked for 30 min with 0.5% BSA in PBS, before incubating for 30 min with 1:250 dilution of rabbit anti-TFEB antibodies (Bethyl Laboratories, TX) in 0.5% BSA. Cells were then washed 3x with 0.5% BSA, incubated with 1:500 dilution of Dylight 488-conjugated donkey anti-rabbit antibodies (Bethyl Laboratories, TX) for 30 min. In some experiments, cells were also incubated for 5 min with 0.4 µg/ml 4',6-diamidino-2-phenylindole (DAPI), washed, and mounted onto glass slides with fluorescent mounting media (DAKO) for imaging.

Fluorescently labelled samples were imaged with one of two microscopy systems. For epifluorescence, we used a 60x oil immersion objective mounted on an Olympus IX83 Inverted Microscope linked to a Hamamatsu ORCA-Flash 4.0 digital camera (Olympus, ON). Images were either used as is or subjected to deconvolution using CellSens Dimension Module (Olympus, ON) with the advanced maximum likelihood estimation algorithm (ADVMLE). Alternatively, confocal imaging was done using a Quorum DisKovery spinning disc confocal microscope system equipped on a Leica DMi8 microscope, with a 63x 1.4 NA oil-immersion objective, and linked to an iXON 897 EMCCD camera. The system was controlled by the Quorum Wave FX powered by MetaMorph software (Quorum Technologies, Guelph, ON).

mCherry-GFP-LC3 autophagy assay

After 24 h of transfection with mCherry-GFP-LC3 plasmid, RAW cells were subjected to an infection assay using both stationary and late-log grown *Salmonella* at an MOI of 100:1. Cells were then followed for 2, 4 and 6 h. At each timepoint, cells were fixed with 4% (v/v) PFA and processed for immunofluorescent staining of *Salmonella* as described above. Images were acquired using a spinning disk confocal microscope as above. To count total autophagosomes,

mCherry positive structures were counted in transfected cells. To count bacteria capture, total internal *Salmonella* in cells were scored and a ratio was formed between LC3 associated bacteria and total bacteria. To assess autophagosome maturation the ratio of mCherry-only structures (no GFP) over total autophagosomes (all mCherry) was done. All conditions shown in Figure 9 and 10 were acquired concurrently. To facilitate analyses and better manage comparisons, these data were split between different graphs.

Image analysis

To quantify nuclear to cytosol TFEB intensity, images were acquired either through single plane acquisition or by acquiring a Z-stack. Epifluorescence Z-stacks were deconvolved to reduce out of focus light and improve contrast and resolution, while single slice images remained untouched. For confocal imaging, background correction was employed. Images were analyzed using ImageJ/FIJI (NIH, MD) or Volocity. For nuclear to cytosolic TFEB ratio, regions of interest were drawn around the nucleus and the cytosol, and the intensities within these regions were then measured. After background subtraction, the ratio of nuclear to cytosol fluorescence was calculated.

Quantitative real-time PCR (qRT-PCR)

RAW macrophages were infected with late-log or stationary phase *Salmonella* for 2, 5 and 20 h as described above. RNA was then extracted using the GeneJet RNA Purification Kit (ThermoFisher Scientific) and transcribed to cDNA using the iScript Reverse Transcription Supermix for RT-qPCR (Bio-Rad). TaqMan gene expression assays were carried out using 50 ng cDNA, the

TaqMan Gene Expression Master Mix (Applied Biosystems) and probes against murine GAPDH, LC3, Cathepsin-D, and Lamp1 (Table 1). Data was normalized to the uninfected, wild-type RAW macrophages for each gene target.

Table 1: TaqMan Gene Expression Probes for each gene

Gene Name	**Assay ID**	**Chromosome Location**
Microtubule-associated protein 1 light chain 3 beta (LC3)	Mm00782868_sH	Chr.8: 121590468 - 121598047
Lysosomal-associated membrane protein 1 (Lamp1)	Mm01217070_m1	Chr.8: 13159134 - 13175338
Cathepsin D	Mm00515586_m1	Chr.7: 142375916 - 142387870
GAPDH	Mm99999915_g1	Chr.6: 125161338 - 125166511

Cell lysates, SDS-PAGE, and Western blotting analysis

After specific cell treatments, whole cell lysates were prepared using 2x Laemmli buffer containing phosSTOP and protease inhibitor cocktail (Roche, Mississauga, ON). Lysates were passed through a 27-gauge needle ten times, then heated at 65 °C for 15 min. For total TFEB levels, lysates were resolved by SDS-PAGE using a 10% acrylamide resolving gel. Proteins were transferred to a PVDF membrane, blocked with 5% BSA, incubated with primary rabbit anti-TFEB antibodies (Bethyl Laboratories, Montgomery, Texas) or primary rabbit anti-β-actin antibodies

(Cell Signaling Technology, Danvers, MA) at a dilution of 1:1000, followed by HRP-conjugated goat anti-rabbit secondary antibodies (Cell Signaling Technology) at 1:5000 dilution. Protein levels were detected via Clarity® enhanced chemiluminescence reagent (Bio-Rad Laboratories, Mississauga, ON) visualized by a ChemiDoc Touch Imaging system (Bio-Rad). Blot intensity quantification was accomplished using ImageLab software (Bio-Rad) and its volumetrics and background subtraction functions. Total TFEB protein levels were normalized to ®-actin.

Phos-tag-PAGE and Western blotting analysis

For analysis of protein phosphorylation, lysates were prepared as described above. Lysates were then run on a 7.5% acrylamide resolving gel containing 50 µM SuperSep Phos-tag (Wako Chemicals, Richmond, Virginia). Proteins were separated at 15 mA and the gel was then washed as per manufacturer's instructions. Proteins were transferred onto a PVDF membrane and visualized as described above. Phosphorylated proteins experience decreased mobility in Phos-tag gels relative to less phosphorylated isoforms. To analyse changes in phosphorylation of TFEB, we marked the migration front of TFEB in resting cells, then measured the volume of TFEB signal upstream and downstream of this front for each condition using ImageLab (Bio-rad). We then measured the ratio of the downstream volume (less phosphorylated) to the upstream volume (more phosphorylated) to assess the degree of TFEB phosphorylation in each condition.

Statistical analyses

All experiments were repeated independently at least three times with the exact number shown in the figure and/or legend. For bacterial survival, each condition had two or three technical replicates. For microscopy analysis, the number of individual cells scored is indicated in

corresponding figure legend. The mean of independent experiments is indicated along with either standard deviation or standard error of the mean, as appropriate. As indicated, sometimes data were normalized to a control condition to account for experimental variation. Unless otherwise stated, data were assumed to be normally distributed and/or have equal variability. Unless otherwise stated, data were subjected to analysis of variance (ANOVA) followed by Tukey's or Sidak's post-hoc test, unless otherwise stated. Data was matched by independent repeats and by concurrent conditions. A p-value of <0.05 was considered significant.

Figure Legends

Figure 1: Stationary-grown *Salmonella* delays TFEB nuclear translocation after phagocytosis. A. Epifluorescence micrographs of fixed RAW macrophages transiently expressing GFP-TFEB and that were given no bacteria (resting) or incubated for 1 h with living *E. coli*, or with living or heat-killed *Salmonella* grown to stationary phase. Samples were stained for external (before permeabilization) and all bacteria (after permeabilization) using anti-*E. coli* or anti-*Salmonella* antibodies. Arrows indicate internalized bacteria. Scale bar = 10 µm. **B.** The nuclear to cytosolic (N/C) fluorescence ratio of GFP-TFEB in macrophages was quantified for the indicated conditions after 1 h of uptake. Means ± SEM were tested using one-way ANOVA test and post-hoc Tukey's test, where *** indicates $p<0.001$. **C** and **D**. GFP-TFEB transfected RAW macrophages engulfed live stationary *E. coli* or *Salmonella* for 1, 4, or 6 h. The N/C fluorescence ratio of GFP-TFEB was then quantified. C and D are different representations of the same data. Data are shown as mean ± SEM from three independent (B) or four independent (C, D) experiments, scoring at least 50 cells for each condition per experiment. For C and D, mean ± SEM are shown and tested using two-way ANOVA test and post-hoc Tukey's test, where *, **, and *** indicate *p*-values of 0.05-0.01, *p*-values of 0.01-0.001, or $p<0.001$, respectively.

Figure 2: Stationary-grown *Salmonella* but not log-phase *Salmonella* delays TFEB activation in macrophages. A. Confocal micrographs of RAW cells expressing GFP-TFEB before, 1 h, or 4 h after engulfing living *E. coli* and *Salmonella* grown to stationary or late log-phase. After uptake, cells were fixed and stained with DAPI and with anti-bacteria antibodies to detect the nucleus and bacteria, respectively. **B**. The N/C fluorescence ratio of GFP-TFEB in macrophages 1 h after engulfment of stationary or late-log bacteria. **C.** The N/C fluorescence ratio of GFP-TFEB in

macrophages 1 h or 4 h after engulfment of stationary grown *E. coli* or *Salmonella.* **D.** The N/C fluorescence ratio of GFP-TFEB in macrophages 1 h or 4 h after engulfment of log-phase grown *E. coli* or *Salmonella.* For B-D, data are shown as mean ± SEM from three independent experiments, scoring 70 cells for each condition per experiment. Means were tested using matched two-way ANOVA test and post-hoc Tukey's test, where *, **, and *** indicate p values of 0.05-0.01, p values of 0.01-0.001, or p<0.001, respectively.

Figure 3: The distribution of endogenous TFEB in macrophages after uptake of viable and non-viable *E. coli and Salmonella*. A. Confocal micrographs of RAW macrophages incubated with living or heat-killed stationary-grown *E. coli* or living or heat-killed *Salmonella* grown to either stationary or late-logarithmic phase. After 1 h, cells were fixed and stained with DAPI (blue) to identify the nucleus, anti-TFEB antibodies (green), and anti-LPS antibodies to identify all bacteria (red). Scale bar = 10 µm. **B.** N/C fluorescence ratio of endogenous TFEB in macrophages subject to indicated conditions. Data are shown as mean ± SEM from three independent experiments, scoring 80 cells for each condition and experiment. Means were tested using one-way ANOVA test with matched data and post-hoc Dunnett's test, where *, **, ***, and **** indicate p values of 0.05-0.01, 0.01-0.001, 0.001-0.0001, or p<0.0001, respectively.

Figure 4. TFEB distribution in HeLa cells after infection with *Salmonella*. A. Confocal images of HeLa cells incubated with living stationary or late-log grown *Salmonella*. After 1 and 4 h post-infection, cells were fixed and stained for external Salmonella with anti-Salmonella serum and far-red secondary antibodies, followed by permeabilization and stained with DAPI (blue) to identify the nucleus, anti-TFEB antibody (green) and anti-*Salmonella* antiserum (red bacteria are internal;

yellow are external). Images represent summed Z stack images. Scale bar = 10 μm. **B.** N/C ratio of endogenous TFEB fluorescence in HeLa cells. Data shown represents mean values ± SEM. Statistical analysis was preformed using matched one-way ANOVA and post-hoc Tukey's test, where * and ** indicate p values of 0.05- 0.01 and 0.01 – 0.001 respectively.

Figure 5: TFEB phosphorylation and protein levels in macrophages after *Salmonella* infection. **A** and **C.** Macrophages engulfed *E. coli* or *Salmonella* grown to stationary or log-phase for 1 or 4 h. Macrophages were then lysed and lysates separated on a Phos-tag SDS-PAGE (A) or standard SDS-PAGE (C), followed by blotting with anti-TFEB antibodies. The loading control was β-actin for both types of electrophoresis. **B** and **D**. The migration front of TFEB separated in Phos-tag gels was measured as indicator of phosphorylation status of TFEB (B) and normalized total TFEB levels relative to β-actin (D). Shown is the mean ±SD analysed from five independent experiments. Data in B was analyzed by a matched one-way ANOVA and Dunnett post-hoc test, while data in D was tested by Friedman one-way ANOVA test and the Dunn's post-hoc test. * and ** indicates a *p*-value of <0.05 and <0.01, respectively.

Figure 6: SPI-I and SPI-II-deficient *Salmonella* do not stall TFEB activation in macrophages. **A.** Confocal images of RAW cells expressing GFP-TFEB (green) 1 h after engulfing wild-type or *invA ssaR Salmonella* grown to stationary or late log-phase. After uptake, cells were fixed and stained with DAPI (blue) and with anti-bacteria antibodies (red). **B**. The N/C fluorescence ratio of GFP-TFEB in macrophages after 1 h engulfment of *Salmonella* strains and grown to indicated phases. Data are shown as mean ± SEM from three independent experiments, scoring at least 70

cells for each condition per experiment. Means were tested using two-way ANOVA test and post-hoc Tukey's test, where * and ** indicate p values of 0.05-0.01 and 0.01-0.001, respectively.

Figure 7: Identification of *Salmonella* mutants that cannot suppress TFEB nuclear translocation in RAW macrophages. A. Epifluorescence micrographs of RAW cells expressing GFP-TFEB 1 h after engulfment of indicated bacteria strains. Cells were fixed and stained for external (cyan) and internal bacteria (red) bacteria with anti-*E. coli* or anti-*Salmonella* antibodies. Arrows point to specific internal bacteria, while full and dotted outlines indicate nucleus and individual cell boundaries. Scale bar represents 10 μm. **B.** N/C ratio of GFP-TFEB in macrophages after engulfment of indicated bacterial strains. **C**. N/C ratio of endogenous TFEB in macrophages after engulfment of indicated bacterial strains. For both B and C, data is shown as mean ± SEM from four independent experiments with approximately 50 cells counted per condition per experiment. Means were tested using one-way ANOVA test and post-hoc Tukey's test, where *, **, and *** indicate p values of 0.05-0.01, p values of 0.01-0.001, or p<0.001, respectively.

Figure 8. mRNA levels of LAMP1, cathepsin D and LC3 during *Salmonella* infection. **A.** Basal expression of LAMP1, cathepsin D and LC3 genes across wildtype, *tfeb*$^{-/-}$ and *tfeb*$^{-/-}$ *tfe3*$^{-/-}$ RAW macrophages normalized to wildtype. **B, D,** and **F.** Relative LAMP1 (B), cathepsin D (D), and LC3 (F) mRNA expression within each cell type infected with either stationary or late-log grown *Salmonella* at indicated times post-infection. **C, E,** and **G.** Comparison of LAMP1(C), cathepsin D (E), and LC3 (G) mRNA expression at 20 h post infection between wild-type, *tfeb*$^{-/-}$ and *tfeb*$^{-/-}$ *tfe3*$^{-/-}$. Data in C, E, and G are the same as 20 h from B, D and F. Data plotted represent means of individual replicates ±SD. Statistical analysis was preformed using matched one-way

ANOVA and post-hoc Tukey's test, where *, ** and *** indicate p values of 0.05- 0.01, 0.01 – 0.001 and 0.001 – 0.0001, respectively.

Figure 9. Autophagy in RAW macrophages during stationary and late-log *Salmonella* infection. A, B, and **C.** Confocal images of wildtype (A), *tfeb*$^{-/-}$ (B), and *tfeb*$^{-/-}$/*tfe3*$^{-/-}$ (C) RAW macrophages transfected with mCherry-GFP-LC3. Cells were subject to stationary or late-log *Salmonella* infection and were fixed at 2, 4 and 6 hours post infection. Cells were also immunofluorescently stained for *Salmonella* using an anti-*Salmonella* antiserum. Panel shows 2- and 6-h post infection images. Scale bar = 12 μm. **D.** Quantification of autophagosomes in resting wildtype, *tfeb*$^{-/-}$, and *tfeb*$^{-/-}$/*tfe3*$^{-/-}$ RAW macrophage. **E, F** and **G.** Comparison of autophagosome numbers between stationary and late-log *Salmonella* infected macrophages over time for each respective cell type. *tfeb*$^{-/-}$ and *tfeb*$^{-/-}$/*tfe3*$^{-/-}$ values are normalized against wildtype resting condition. Plotted values represent mean values per replicate and ±SEM. For D, statistical analysis was done using one-way ANOVA and Friedman's multiple comparisons. Statistical analysis for **E-G** was preformed using matched two-way ANOVA and post-hoc Tukey's test, where *, ** and *** indicate p values of 0.05- 0.01, 0.01 – 0.001 and 0.001 – 0.0001, respectively.

Figure 10. Autophagosome maturation and xenophagy bacterial capture in RAW macrophages during Salmonella infection. **A.** Ratio of mature over total autophagosomes in resting wildtype, *tfeb*$^{-/-}$, and *tfeb*$^{-/-}$/*tfe3*$^{-/-}$ RAW macrophages normalized to wildtype. **B.** Ratio of mature to total autophagosomes during stationary or late-log infection in wildtype, *tfeb*$^{-/-}$, and *tfeb*$^{-/-}$/*tfe3*$^{-/-}$ RAW macrophages. **C.** Ratio of LC3-labelled bacteria over total bacteria during infection in each macrophage genotype. Data plotted represent mean values and ±SEM from n=5

independent experiments. Statistical analysis was preformed using matched one-way ANOVA and post-hoc Tukey's test.

Figure 11. *E. coli* and *Salmonella* survival in wild-type, *tfeb*$^{-/-}$ macrophages, and HeLA-TKO cells. A and **B**. Wild-type and *tfeb*$^{-/-}$ RAW macrophages were allowed to phagocytose live *E. coli* (A) or *Salmonella* (B) for 1 h, followed with gentamycin to kill external bacteria. One macrophage population was immediately lysed and bacteria were plated to count CFUs as an estimate of bacterial uptake. A second population of macrophages was incubated for 4 h with low gentamycin, then lysed, and bacteria plated to count CFUs as indicator of acute bacterial survival in macrophages. Data is shown as percent survival by taking the ratio of CFUs after 4 h of incubation relative to CFUs formed after 1 h incubation (uptake). **C.** Wild-type and *tfeb*$^{-/-}$ *tfe3*$^{-/-}$ RAW macrophages were allowed to engulf stationary and late-logarithmic grown *Salmonella*. **D.** Infection of wild-type HeLa and *tfeb*$^{-/-}$ *tfe3*$^{-/-}$ *mitf*$^{-/-}$ HeLa (HeLa-TKO) cells as described in C. Infections were followed for 4 and 20 h post infection. Percent survival was determined as described above. Data are shown as the mean ± SD from four (D) or six (E) independent experiments. Data in A and B were statistically analyzed by paired Student's t-test, while data in C and D were tested by matched two-way ANOVA and Šidák post-hoc test. P values are disclosed for survival assays.

Figure 12: Ectopic activation of TFEB enhances *Salmonella* killing in macrophages in a TFEB-dependent manner. A and **B**. Wild-type and *tfeb*$^{-/-}$ RAW macrophages were left untreated or pre-activated with IgG-opsonized beads as described in methods and then allowed to engulf live *E.coli* (A) or *Salmonella* (B). Percent survival of *E. coli* (A) or *Salmonella* (B) was determined

by comparing number of CFUs between initial uptake and 3 h post uptake. Shown is the average ± STD from n=8 independent experiments. **C**. Cells were pretreated with 20 nM apilimod or DMSO vehicle for 1 h and maintained through the infection with stationary or late-logarithmic *Salmonella*. Percent survival of bacteria was measured by comparing the number of CFU at the end of 4 h chase with CFUs from initial uptake (1 h) as described in methods. Shown is the mean and standard deviation from n=3 independent experiments. A-C: Data was analyzed by matched two-way ANOVA and Šidák's post-hoc test. Actual p values are shown for survival experiments

Funding Acknowledgement

This research was made possible with financial support to R.J.B. from the Canada Research Chairs Program (950-232333), The Early Researcher Award from the Government of Ontario (ER13-09-042), The John Evans LOF Program from the Canada Foundation for Innovation (32957), the Research Instruments and Innovation Grant Program from Natural Sciences and Engineering Council of Canada (EQPEQ 458501-2014), and contributions from Toronto Metropolitan University (Formerly Ryerson University). The J.B.M. lab contributions was funded by Discovery Program from the Natural Sciences and Engineering Council of Canada (RGPIN/04679-2015).

References

Ammanathan, V., Mishra, P., Chavalmane, A.K., Muthusamy, S., Jadhav, V., Siddamadappa, C., and Manjithaya, R. (2020) Restriction of intracellular Salmonella replication by restoring TFEB-mediated xenophagy. *Autophagy* **16**: 1584–1597.

Axline, S.G., and Cohn, Z.A. (1970) In vitro induction of lysosomal enzymes by phagocytosis. *J Exp Med* **131**: 1239–1260.

Bao, J., Zheng, L., Zhang, Q., Li, X., Zhang, X., Li, Z., *et al.* (2016) Deacetylation of TFEB promotes fibrillar Aβ degradation by upregulating lysosomal biogenesis in microglia. *Protein Cell* **7**: 417–433.

Benjamin, W.H., Posey, B.S., and Briles, D.E. (1986) Effects of in vitro growth phase on the pathogenesis of Salmonella typhimurium in mice. *J Gen Microbiol* **132**: 1283–1295.

Bijlsma, J.J.E., and Groisman, E.A. (2005) The PhoP/PhoQ system controls the intramacrophage type three secretion system of Salmonella enterica. *Mol Microbiol* **57**: 85–96.

Bouvier, G., Benoliel, A.M., Foa, C., and Bongrand, P. (1994) Relationship between phagosome acidification, phagosome-lysosome fusion, and mechanism of particle ingestion. *J Leukoc Biol* **55**: 729–34.

Brady, O.A., Martina, J.A., and Puertollano, R. (2018) Emerging roles for TFEB in the immune response and inflammation. *Autophagy* **14**: 181–189.

Brandes, D., and Anton, E. (1969) An electron microscopic cytochemical study of macrophages during uterine involution. *J Cell Biol* **41**: 450–461.

Bravo, D., Silva, C., Carter, J.A., Hoare, A., Álvarez, S.A., Blondel, C.J., *et al.* (2008) Growth-phase regulation of lipopolysaccharide O-antigen chain length influences serum resistance in serovars of Salmonella. *J Med Microbiol* **57**: 938–946.

Brumell, J.H., Kujat-Choy, S., Brown, N.F., Vallance, B.A., Knodler, L.A., and Finlay, B.B. (2003) SopD2 is a novel type III secreted effector of Salmonella typhimurium that targets late endocytic compartments upon delivery into host cells. *Traffic* **4**: 36–48.

Bruno, V.M., Hannemann, S., Lara-Tejero, M., Flavell, R.A., Kleinstein, S.H., and Galán, J.E. (2009) Salmonella Typhimurium Type III Secretion Effectors Stimulate Innate Immune Responses in Cultured Epithelial Cells. *PLOS Pathog* **5**: e1000538.

Bustamante, V.H., Martínez, L.C., Santana, F.J., Knodler, L.A., Steele-Mortimer, O., and Puente, J.L. (2008) HilD-mediated transcriptional cross-talk between SPI-1 and SPI-2. *Proc Natl Acad Sci U S A* **105**: 14591–14596.

904 Choy, C.H., Saffi, G., Gray, M.A., Wallace, C., Dayam, R.M., Ou, Z.Y.A., *et al.* (2018) Lysosome
905 enlargement during inhibition of the lipid kinase PIKfyve proceeds through lysosome
906 coalescence. *J Cell Sci* **131**: jcs213587.

907 Cirillo, D.M., Valdivia, R.H., Monack, D.M., and Falkow, S. (1998) Macrophage-dependent
908 induction of the Salmonella pathogenicity island 2 type III secretion system and its role in
909 intracellular survival. *Mol Microbiol* **30**: 175–188.

910 Collazo, C.M., and Galán, J.E. (1997) The invasion-associated type III system of Salmonella
911 typhimurium directs the translocation of Sip proteins into the host cell. *Mol Microbiol* **24**: 747–
912 756.

913 D'Costa, V.M., Braun, V., Landekic, M., Shi, R., Proteau, A., McDonald, L., *et al.* (2015) Salmonella
914 Disrupts Host Endocytic Trafficking by SopD2-Mediated Inhibition of Rab7. *Cell Rep* **12**: 1508–
915 1518.

916 D'Costa, V.M., Coyaud, E., Boddy, K.C., Laurent, E.M.N., St-Germain, J., Li, T., *et al.* (2019) BioID
917 screen of Salmonella type 3 secreted effectors reveals host factors involved in vacuole positioning
918 and stability during infection. *Nat Microbiol* **4**: 2511–2522.

919 Deiwick, J., Nikolaus, T., Erdogan, S., and Hensel, M. (1999) Environmental regulation of
920 Salmonella pathogenicity island 2 gene expression. *Mol Microbiol* **31**: 1759–1773.

921 Drecktrah, D., Knodler, L.A., Ireland, R., and Steele-Mortimer, O. (2006) The mechanism of
922 Salmonella entry determines the vacuolar environment and intracellular gene expression. *Traffic*
923 **7**: 39–51.

924 Dumont, A., Boucrot, E., Drevensek, S., Daire, V., Gorvel, J.-P., Poüs, C., *et al.* (2010) SKIP, the Host
925 Target of the Salmonella Virulence Factor SifA, Promotes Kinesin-1-Dependent Vacuolar
926 Membrane Exchanges. *Traffic* **11**: 899–911.

927 Figueira, R., Watson, K.G., Holden, D.W., and Helaine, S. (2013) Identification of Salmonella
928 Pathogenicity Island-2 Type III Secretion System Effectors Involved in Intramacrophage
929 Replication of S. enterica Serovar Typhimurium: Implications for Rational Vaccine Design. *mBio*
930 **4**: e00065-13.

931 Flannagan, R.S., Jaumouillé, V., and Grinstein, S. (2012) The cell biology of phagocytosis. *Annu*
932 *Rev Pathol* **7**: 61–98.

933 Fountain, A., Inpanathan, S., Alves, P., Verdawala, M.B., and Botelho, R.J. (2021) Phagosome
934 maturation in macrophages: Eat, digest, adapt, and repeat. *Adv Biol Regul* **82**: 100832.

935 Fratti, R.A., Backer, J.M., Gruenberg, J., Corvera, S., and Deretic, V. (2001) Role of
936 phosphatidylinositol 3-kinase and Rab5 effectors in phagosomal biogenesis and mycobacterial
937 phagosome maturation arrest. *J Cell Biol* **154**: 631–644.

938 Geddes, K., Worley, M., Niemann, G., and Heffron, F. (2005) Identification of new secreted
939 effectors in Salmonella enterica serovar typhimurium. *Infect Immun* **73**: 6260–6271.

940 Gog, J.R., Murcia, A., Osterman, N., Restif, O., McKinley, T.J., Sheppard, M., *et al.* (2012) Dynamics
941 of Salmonella infection of macrophages at the single cell level. *J R Soc Interface* **9**: 2696–2707.

942 Gray, M.A., Choy, C.H., Dayam, R.M., Ospina-Escobar, E., Somerville, A., Xiao, X., *et al.* (2016)
943 Phagocytosis Enhances Lysosomal and Bactericidal Properties by Activating the Transcription
944 Factor TFEB. *Curr Biol* **26**: 1955–1964.

945 Harrison, R.E., Bucci, C., Vieira, O.V., Schroer, T.A., and Grinstein, S. (2003) Phagosomes Fuse with
946 Late Endosomes and/or Lysosomes by Extension of Membrane Protrusions along Microtubules:
947 Role of Rab7 and RILP. *Mol Cell Biol* **23**: 6494–6506.

948 Heijden, J. van der, Bosman, E.S., Reynolds, L.A., and Finlay, B.B. (2015) Direct measurement of
949 oxidative and nitrosative stress dynamics in Salmonella inside macrophages. *Proc Natl Acad Sci*
950 *U S A* **112**: 560–565.

951 Hensel, M., Shea, J.E., Waterman, S.R., Mundy, R., Nikolaus, T., Banks, G., *et al.* (1998) Genes
952 encoding putative effector proteins of the type III secretion system of Salmonella pathogenicity
953 island 2 are required for bacterial virulence and proliferation in macrophages. *Mol Microbiol* **30**:
954 163–74.

955 Hersch, S.J., and Navarre, W.W. (2020) The Salmonella LysR Family Regulator RipR Activates the
956 SPI-13-Encoded Itaconate Degradation Cluster. *Infect Immun* **88**: e00303-20.

957 Hipolito, V.E.B., Diaz, J.A., Tandoc, K.V., Oertlin, C., Ristau, J., Chauhan, N., *et al.* (2019) Enhanced
958 translation expands the endo-lysosome size and promotes antigen presentation during
959 phagocyte activation. *PLoS Biol* **17**: e3000535.

960 Hipolito, V.E.B., Ospina-Escobar, E., and Botelho, R.J. (2018) Lysosome remodelling and
961 adaptation during phagocyte activation. *Cell Microbiol* **20**: e12824.

962 Ibarra, J.A., Knodler, L.A., Sturdevant, D.E., Virtaneva, K., Carmody, A.B., Fischer, E.R., *et al.* (2010)
963 Induction of Salmonella pathogenicity island 1 under different growth conditions can affect
964 Salmonella-host cell interactions in vitro. *Microbiology* **156**: 1120–33.

965 Inpanathan, S., and Botelho, R.J. (2019) The Lysosome Signaling Platform: Adapting With the
966 Times. *Front Cell Dev Biol* **7**: 113.

967 Irazoqui, J.E. (2020) Key Roles of MiT Transcription Factors in Innate Immunity and Inflammation.
968 *Trends Immunol* **41**: 157–171.

969 Jennings, E., Thurston, T.L.M., and Holden, D.W. (2017) Salmonella SPI-2 Type III Secretion System
970 Effectors: Molecular Mechanisms And Physiological Consequences. *Cell Host Microbe* **22**: 217–
971 231.

972 Kielian, M.C., and Cohn, Z.A. (1980) Phagosome-lysosome fusion. Characterization of intracellular
973 membrane fusion in mouse macrophages. *J Cell Biol* **85**: 754–65.

974 Kim, G.H.E., Dayam, R.M., Prashar, A., Terebiznik, M., and Botelho, R.J. (2014) PIKfyve inhibition
975 interferes with phagosome and endosome maturation in macrophages. *Traffic* **15**: 1143–63.

976 Kim, J.-S., Liu, L., Davenport, B., Kant, S., Morrison, T.E., and Vazquez-Torres, A. (2022) Oxidative
977 stress activates transcription of Salmonella pathogenicity island-2 genes in macrophages. *J Biol*
978 *Chem* **298**: 102130.

979 Kurtz, J.R., Nieves, W., Bauer, D.L., Israel, K.E., Adcox, H.E., Gunn, J.S., *et al.* (2020) Salmonella
980 Persistence and Host Immunity Are Dictated by the Anatomical Microenvironment. *Infect Immun*
981 **88**: e00026-20.

982 Lathrop, S.K., Binder, K.A., Starr, T., Cooper, K.G., Chong, A., Carmody, A.B., and Steele-Mortimer,
983 O. (2015) Replication of Salmonella enterica Serovar Typhimurium in Human Monocyte-Derived
984 Macrophages. *Infect Immun* **83**: 2661–2671.

985 Levin, R., Grinstein, S., and Canton, J. (2016) The life cycle of phagosomes: formation, maturation,
986 and resolution. *Immunol Rev* **273**: 156–179.

987 Lou, L., Zhang, P., Piao, R., and Wang, Y. (2019) Salmonella Pathogenicity Island 1 (SPI-1) and Its
988 Complex Regulatory Network. *Front Cell Infect Microbiol* **9**: 270.

989 Lundberg, U., Vinatzer, U., Berdnik, D., Gabain, A. von, and Baccarini, M. (1999) Growth Phase-
990 Regulated Induction ofSalmonella-Induced Macrophage Apoptosis Correlates with Transient
991 Expression of SPI-1 Genes. *J Bacteriol* **181**: 3433–3437.

992 Martina, J.A., Chen, Y., Gucek, M., and Puertollano, R. (2012) MTORC1 functions as a
993 transcriptional regulator of autophagy by preventing nuclear transport of TFEB. *Autophagy* **8**:
994 903–14.

995 Martin-Orozco, N., Touret, N., Zaharik, M.L., Park, E., Kopelman, R., Miller, S., *et al.* (2006)
996 Visualization of vacuolar acidification-induced transcription of genes of pathogens inside
997 macrophages. *Mol Biol Cell* **17**: 498–510.

998 McEwan, D.G., Richter, B., Claudi, B., Wigge, C., Wild, P., Farhan, H., *et al.* (2015) PLEKHM1
999 Regulates Salmonella-Containing Vacuole Biogenesis and Infection. *Cell Host Microbe* **17**: 58–71.

1000 Medina, D.L., Di Paola, S., Peluso, I., Armani, A., De Stefani, D., Venditti, R., *et al.* (2015) Lysosomal
1001 calcium signalling regulates autophagy through calcineurin and TFEB. *Nat Cell Biol* **17**: 288–299.

1002 Mrakovic, A., Kay, J.G., Furuya, W., Brumell, J.H., and Botelho, R.J. (2012) Rab7 and Arl8 GTPases
1003 are Necessary for Lysosome Tubulation in Macrophages. *Traffic* **13**: 1667–1679.

1004 Mulder, D.T., Cooper, C.A., and Coombes, B.K. (2012) Type VI secretion system-associated gene
1005 clusters contribute to pathogenesis of Salmonella enterica serovar Typhimurium. *Infect Immun*
1006 **80**: 1996–2007.

1007 Nagy, Z., Comer, S., and Smolenski, A. (2018) Analysis of Protein Phosphorylation Using Phos-Tag
1008 Gels. *Curr Protoc Protein Sci* **93**: e64.

1009 Najibi, M., Honwad, H.H., Moreau, J.A., Becker, S.M., and Irazoqui, J.E. (2022) A NOVEL
1010 NOX/PHOX-CD38-NAADP-TFEB AXIS IMPORTANT FOR MACROPHAGE ACTIVATION DURING
1011 BACTERIAL PHAGOCYTOSIS. *Autophagy* **18**: 124–141.

1012 Najibi, M., Labed, S.A., Visvikis, O., and Irazoqui, J.E. (2016) An Evolutionarily Conserved PLC-PKD-
1013 TFEB Pathway for Host Defense. *Cell Rep* **15**: 1728–1742.

1014 Nezich, C.L., Wang, C., Fogel, A.I., and Youle, R.J. (2015) MiT/TFE transcription factors are
1015 activated during mitophagy downstream of Parkin and Atg5. *J Cell Biol* **210**: 435–450.

1016 Nguyen, J.A., and Yates, R.M. (2021) Better Together: Current Insights Into Phagosome-Lysosome
1017 Fusion. *Front Immunol* **12**: 636078.

1018 Pastore, N., Brady, O.A., Diab, H.I., Martina, J.A., Sun, L., Huynh, T., *et al.* (2016) TFEB and TFE3
1019 cooperate in the regulation of the innate immune response in activated macrophages.
1020 *Autophagy* **12**: 1240–1258.

1021 Patel, J.C., and Galán, J.E. (2005) Manipulation of the host actin cytoskeleton by Salmonella — all
1022 in the name of entry. *Curr Opin Microbiol* **8**: 10–15.

1023 Pei, G., Repnik, U., Griffiths, G., and Gutierrez, M.G. (2014) Identification of an immune-regulated
1024 phagosomal Rab cascade in macrophages. *J Cell Sci* **127**: 2071–2082.

1025 Portaliou, A.G., Tsolis, K.C., Loos, M.S., Zorzini, V., and Economou, A. (2016) Type III Secretion:
1026 Building and Operating a Remarkable Nanomachine. *Trends Biochem Sci* **41**: 175–189.

1027 Prost, L.R., and Miller, S.I. (2008) The Salmonellae PhoQ sensor: mechanisms of detection of
1028 phagosome signals. *Cell Microbiol* **10**: 576–582.

1029 Puertollano, R., Ferguson, S.M., Brugarolas, J., and Ballabio, A. (2018) The complex relationship
1030 between TFEB transcription factor phosphorylation and subcellular localization. *EMBO J* **37**:
1031 e98804.

1032 Raffatellu, M., Wilson, R.P., Chessa, D., Andrews-Polymenis, H., Tran, Q.T., Lawhon, S., *et al.*
1033 (2005) SipA, SopA, SopB, SopD, and SopE2 contribute to Salmonella enterica serotype
1034 typhimurium invasion of epithelial cells. *Infect Immun* **73**: 146–154.

1035 Rao, S., Xu, T., Xia, Y., and Zhang, H. (2020) Salmonella and S. aureus Escape From the Clearance
1036 of Macrophages via Controlling TFEB. *Front Microbiol* **11**: 573844.

1037 Roczniak-Ferguson, A., Petit, C.S., Froehlich, F., Qian, S., Ky, J., Angarola, B., *et al.* (2012) The
1038 transcription factor TFEB links mTORC1 signaling to transcriptional control of lysosome
1039 homeostasis. *Sci Signal* **5**: ra42.

1040 Sachdeva, K., Goel, M., Sudhakar, M., Mehta, M., Raju, R., Raman, K., *et al.* (2020) Mycobacterium
1041 tuberculosis (Mtb) lipid mediated lysosomal rewiring in infected macrophages modulates
1042 intracellular Mtb trafficking and survival. *J Biol Chem* **295**: 9192–9210.

1043 Sasikaran, J., Ziemski, M., Zadora, P.K., Fleig, A., and Berg, I.A. (2014) Bacterial itaconate
1044 degradation promotes pathogenicity. *Nat Chem Biol* **10**: 371–377.

1045 Schuster, E.-M., Epple, M.W., Glaser, K.M., Mihlan, M., Lucht, K., Zimmermann, J.A., *et al.* (2022)
1046 TFEB induces mitochondrial itaconate synthesis to suppress bacterial growth in macrophages.
1047 *Nat Metab* **4**: 856–866.

1048 Settembre, C., De Cegli, R., Mansueto, G., Saha, P.K., Vetrini, F., Visvikis, O., *et al.* (2013a) TFEB
1049 controls cellular lipid metabolism through a starvation-induced autoregulatory loop. *Nat Cell Biol*
1050 **15**: 647–58.

1051 Settembre, C., De Cegli, R., Mansueto, G., Saha, P.K., Vetrini, F., Visvikis, O., *et al.* (2013b) TFEB
1052 controls cellular lipid metabolism through a starvation-induced autoregulatory loop. *Nat Cell Biol*
1053 **15**: 647–58.

1054 Settembre, C., Di Malta, C., Polito, V.A., Garcia Arencibia, M., Vetrini, F., Erdin, S., *et al.* (2011)
1055 TFEB links autophagy to lysosomal biogenesis. *Science* **332**: 1429–33.

1056 Settembre, C., Zoncu, R., Medina, D.L., Vetrini, F., Erdin, S.S., Erdin, S.S., *et al.* (2012) A lysosome-
1057 to-nucleus signalling mechanism senses and regulates the lysosome via mTOR and TFEB. *Eur Mol*
1058 *Biol Organ J* **31**: 1095–108.

1059 Shea, J.E., Beuzon, C.R., Gleeson, C., Mundy, R., and Holden, D.W. (1999) Influence of the
1060 Salmonella typhimuriumPathogenicity Island 2 Type III Secretion System on Bacterial Growth in
1061 the Mouse. *Infect Immun* **67**: 213–219.

1062 Song, M., Kim, H.-J., Kim, E.Y., Shin, M., Lee, H.C., Hong, Y., *et al.* (2004) ppGpp-dependent
1063 Stationary Phase Induction of Genes on Salmonella Pathogenicity Island 1*. *J Biol Chem* **279**:
1064 34183–34190.

1065 Swanson, J., Burke, E., and Silverstein, S.C. (1987) Tubular lysosomes accompany stimulated
1066 pinocytosis in macrophages. *J Cell Biol* **104**: 1217–1222.

1067 Terebiznik, M.R., Vieira, O.V., Marcus, S.L., Slade, A., Yip, C.M., Trimble, W.S., *et al.* (2002)
1068 Elimination of host cell PtdIns(4,5)P(2) by bacterial SigD promotes membrane fission during
1069 invasion by Salmonella. *Nat Cell Biol* **4**: 766–773.

1070 Tsunemi, T., Ashe, T.D., Morrison, B.E., Soriano, K.R., Au, J., Roque, R.A.V., *et al.* (2012) PGC-1α
1071 rescues Huntington's disease proteotoxicity by preventing oxidative stress and promoting TFEB
1072 function. *Sci Transl Med* **4**: 142ra97.

1073 Vieira, O.V., Bucci, C., Harrison, R.E., Trimble, W.S., Lanzetti, L., Gruenberg, J., *et al.* (2003)
1074 Modulation of Rab5 and Rab7 recruitment to phagosomes by phosphatidylinositol 3-kinase. *Mol*
1075 *Cell Biol* **23**: 2501–14.

1076 Visvikis, O., Ihuegbu, N., Labed, S.A.A., Luhachack, L.G.G., Alves, A.-M.F.M.F.M.F., Wollenberg,
1077 A.C.C., *et al.* (2014) Innate host defense requires TFEB-mediated transcription of cytoprotective
1078 and antimicrobial genes. *Immunity* **40**: 896–909.

1079 Vyas, J.M., Kim, Y.-M., Artavanis-Tsakonas, K., Love, J.C., Van der Veen, A.G., and Ploegh, H.L.
1080 (2007) Tubulation of class II MHC compartments is microtubule dependent and involves multiple
1081 endolysosomal membrane proteins in primary dendritic cells. *J Immunol* **178**: 7199–210.

1082 Westman, J., Walpole, G.F.W., Kasper, L., Xue, B.Y., Elshafee, O., Hube, B., and Grinstein, S. (2020)
1083 Lysosome Fusion Maintains Phagosome Integrity during Fungal Infection. *Cell Host Microbe* **28**:
1084 798-812.e6.

1085 Zhang, Z., Chen, C., Yang, F., Zeng, Y.-X., Sun, P., Liu, P., and Li, X. (2022) Itaconate is a lysosomal
1086 inducer that promotes antibacterial innate immunity. *Mol Cell* S1097-2765(22)00443–9.

1087

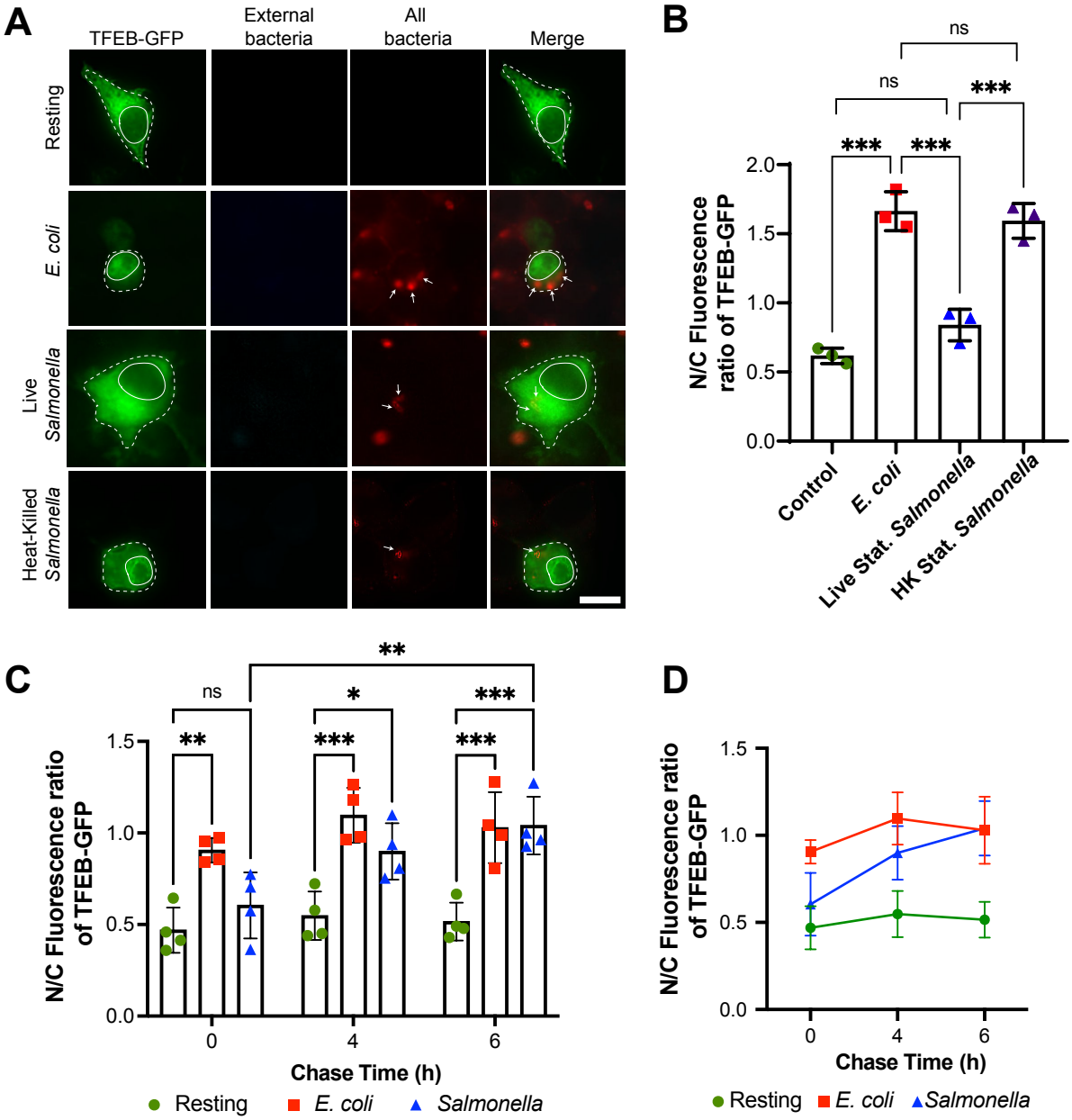
A
TFEB-GFP
External bacteria
All bacteria
Merge
Resting
E. coli
Live Salmonella
Heat-Killed Salmonella
B
ns
ns
***
***
***
N/C Fluorescence ratio of TFEB-GFP
2.0
1.5
1.0
0.5
0.0
Control
E. coli
Live Stat. Salmonella
HK Stat. Salmonella
C
**
ns
*
***
**
***
***
N/C Fluorescence ratio of TFEB-GFP
1.5
1.0
0.5
0.0
0
4
6
Chase Time (h)
Resting
E. coli
Salmonella
D
N/C Fluorescence ratio of TFEB-GFP
1.5
1.0
0.5
0.0
0
4
6
Chase Time (h)
Resting
E. coli
Salmonella

Figure 1

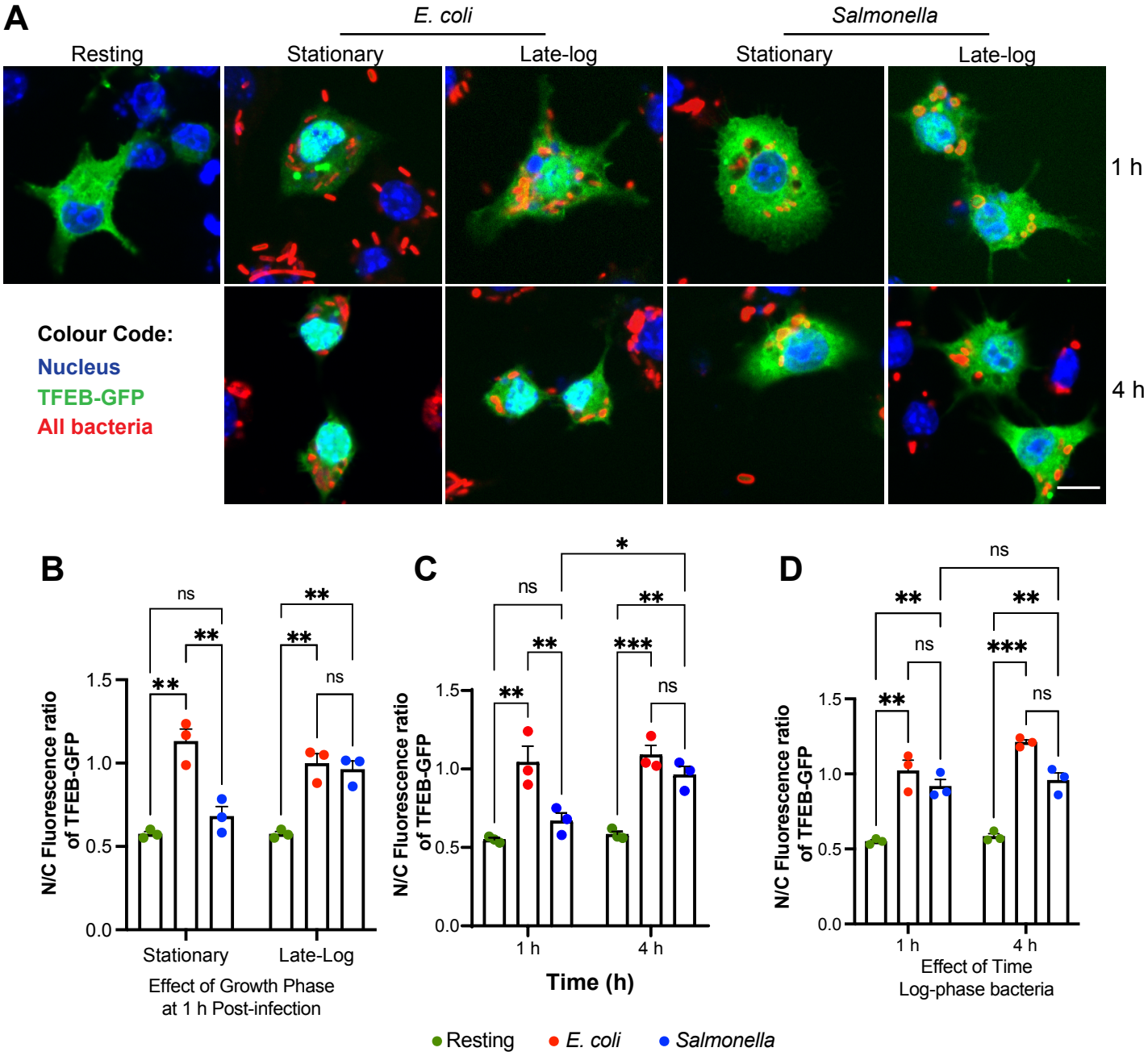
A
E. coli
Salmonella
Resting
Stationary
Late-log
Stationary
Late-log
1 h
4 h
Colour Code:
Nucleus
TFEB-GFP
All bacteria
B
N/C Fluorescence ratio of TFEB-GFP
Stationary
Late-Log
Effect of Growth Phase at 1 h Post-infection
C
Time (h)
1 h
4 h
D
Effect of Time Log-phase bacteria
Resting
E. coli
Salmonella

Figure 2

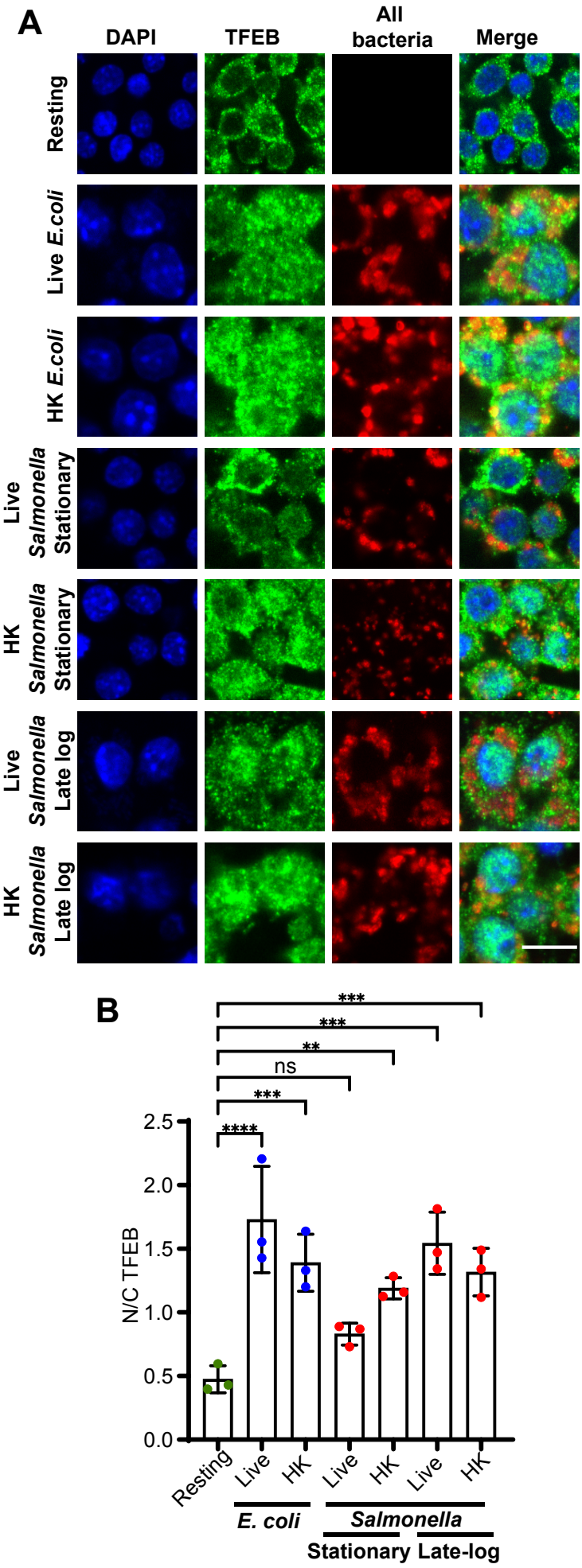
A
DAPI
TFEB
All bacteria
Merge
Resting
Live E.coli
HK E.coli
Live Salmonella Stationary
HK Salmonella Stationary
Live Salmonella Late log
HK Salmonella Late log
B
***
***
**
ns
***
****
2.5
2.0
1.5
1.0
0.5
0.0
N/C TFEB
Resting
Live
HK
Live
HK
Live
HK
E. coli
Salmonella
Stationary
Late-log

Figure 3

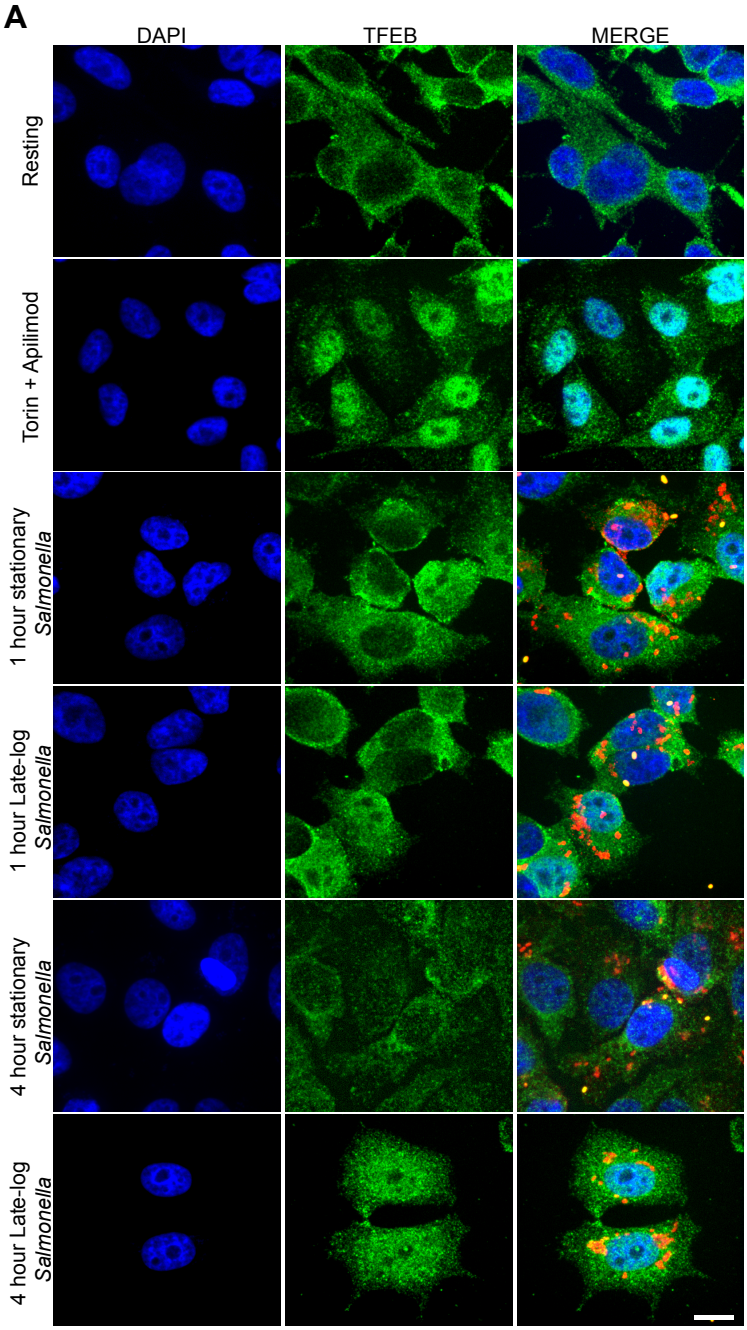
A
DAPI
TFEB
MERGE
Resting
Torin + Apilimod
1 hour stationary Salmonella
1 hour Late-log Salmonella
4 hour stationary Salmonella
4 hour Late-log Salmonella

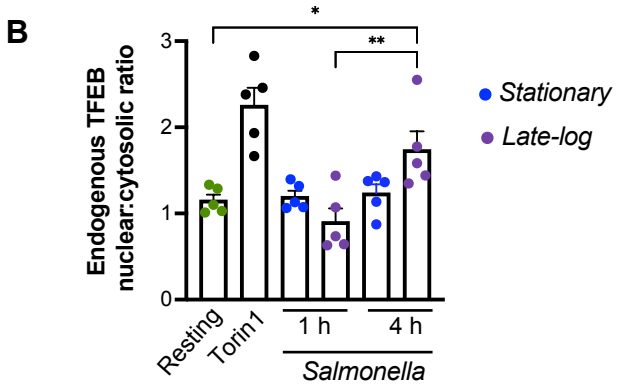
B
Endogenous TFEB nuclear:cytosolic ratio
0
1
2
3
*
**
Resting
Torin1
1 h
4 h
Salmonella
Stationary
Late-log

Figure 4

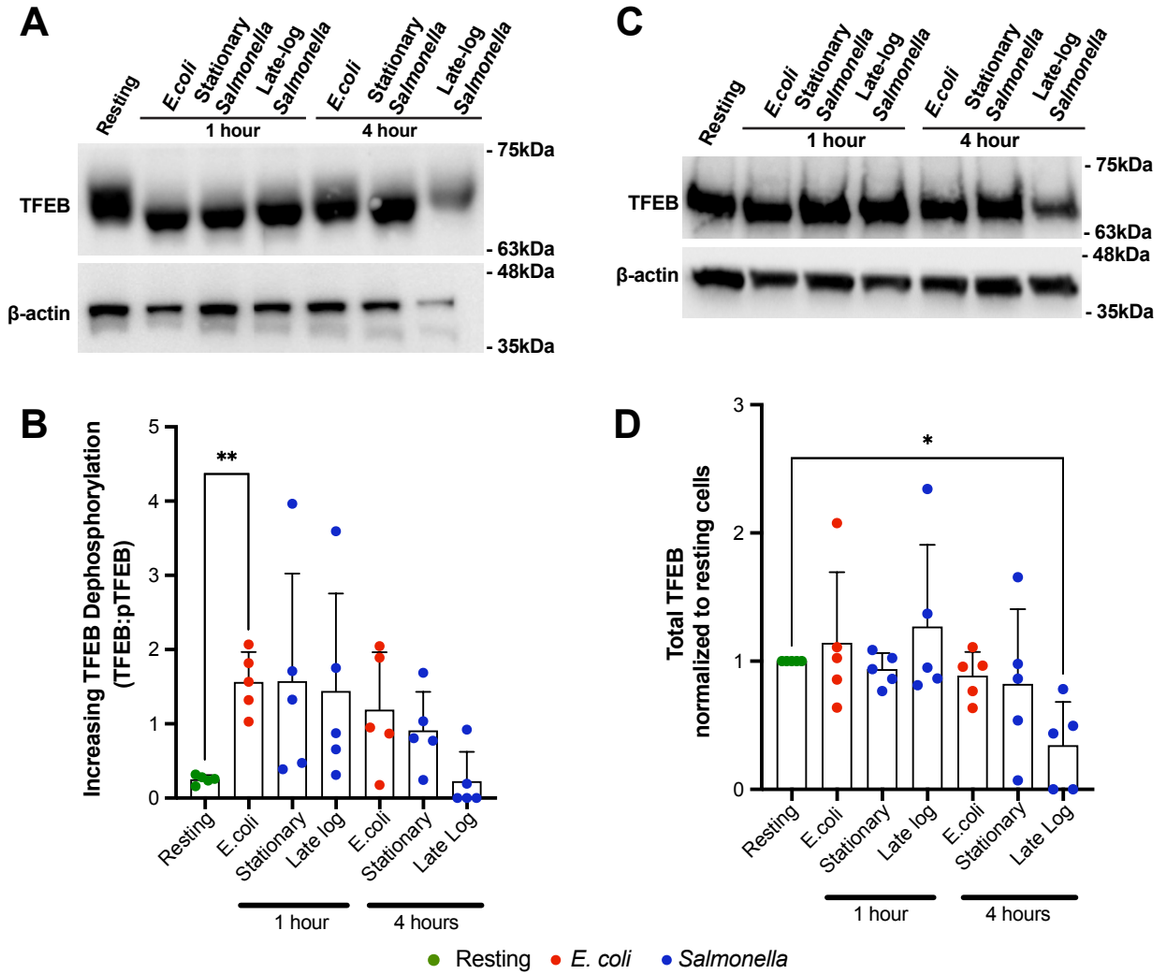
A
Resting
E.coli
Stationary Salmonella
Late-log Salmonella
1 hour
4 hour
TFEB
β-actin
- 75kDa
- 63kDa
- 48kDa
- 35kDa
C
B
Increasing TFEB Dephosphorylation (TFEB:pTFEB)
**
Resting
E.coli
Stationary
Late log
Late Log
1 hour
4 hours
D
Total TFEB normalized to resting cells
*
Resting
E. coli
Salmonella

Figure 5

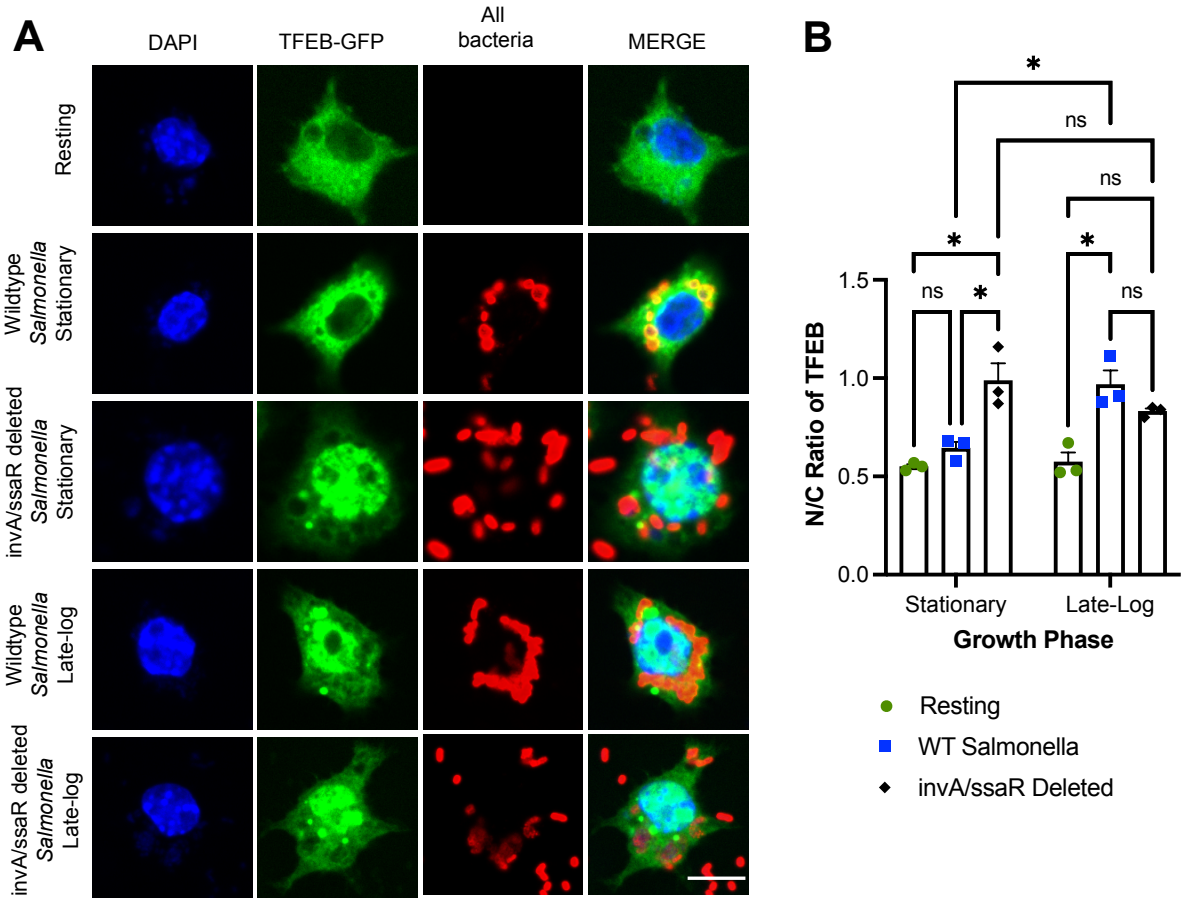
A
DAPI
TFEB-GFP
All bacteria
MERGE
Resting
Wildtype Salmonella Stationary
invA/ssaR deleted Salmonella Stationary
Wildtype Salmonella Late-log
invA/ssaR deleted Salmonella Late-log
B
N/C Ratio of TFEB
1.5
1.0
0.5
0.0
Stationary
Late-Log
Growth Phase
ns
*
Resting
WT Salmonella
invA/ssaR Deleted

Figure 6

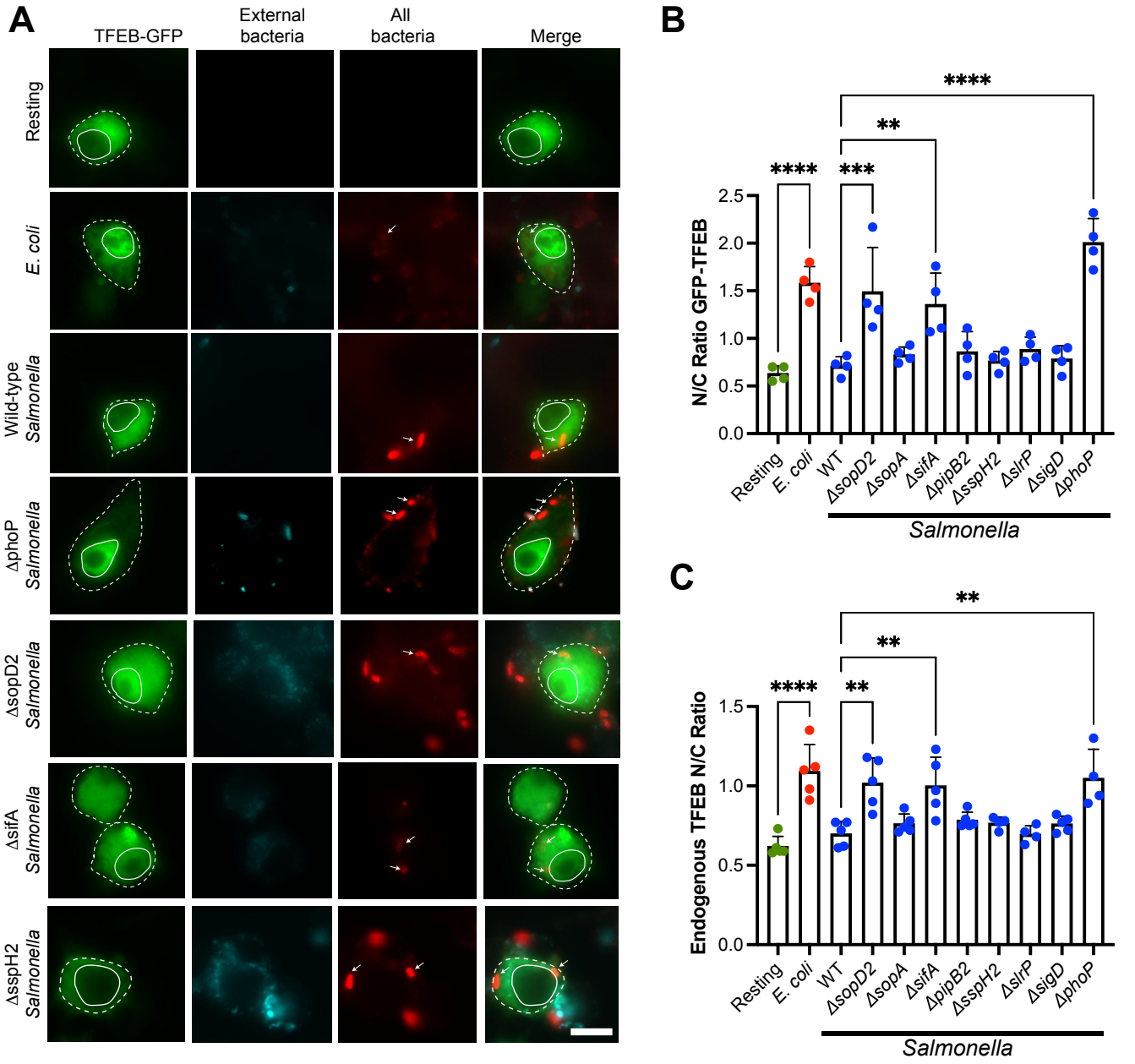
A
TFEB-GFP
External bacteria
All bacteria
Merge
Resting
E. coli
Wild-type Salmonella
ΔphoP Salmonella
ΔsopD2 Salmonella
ΔsifA Salmonella
ΔsspH2 Salmonella
B
N/C Ratio GFP-TFEB
2.5
2.0
1.5
1.0
0.5
0.0
****
***
**
****
Resting
E. coli
WT
ΔsopD2
ΔsopA
ΔsifA
ΔpipB2
ΔsspH2
ΔslrP
ΔsigD
ΔphoP
Salmonella
C
Endogenous TFEB N/C Ratio
1.5
1.0
0.5
0.0
****
**
**
**
Resting
E. coli
WT
ΔsopD2
ΔsopA
ΔsifA
ΔpipB2
ΔsspH2
ΔslrP
ΔsigD
ΔphoP
Salmonella

Figure 7

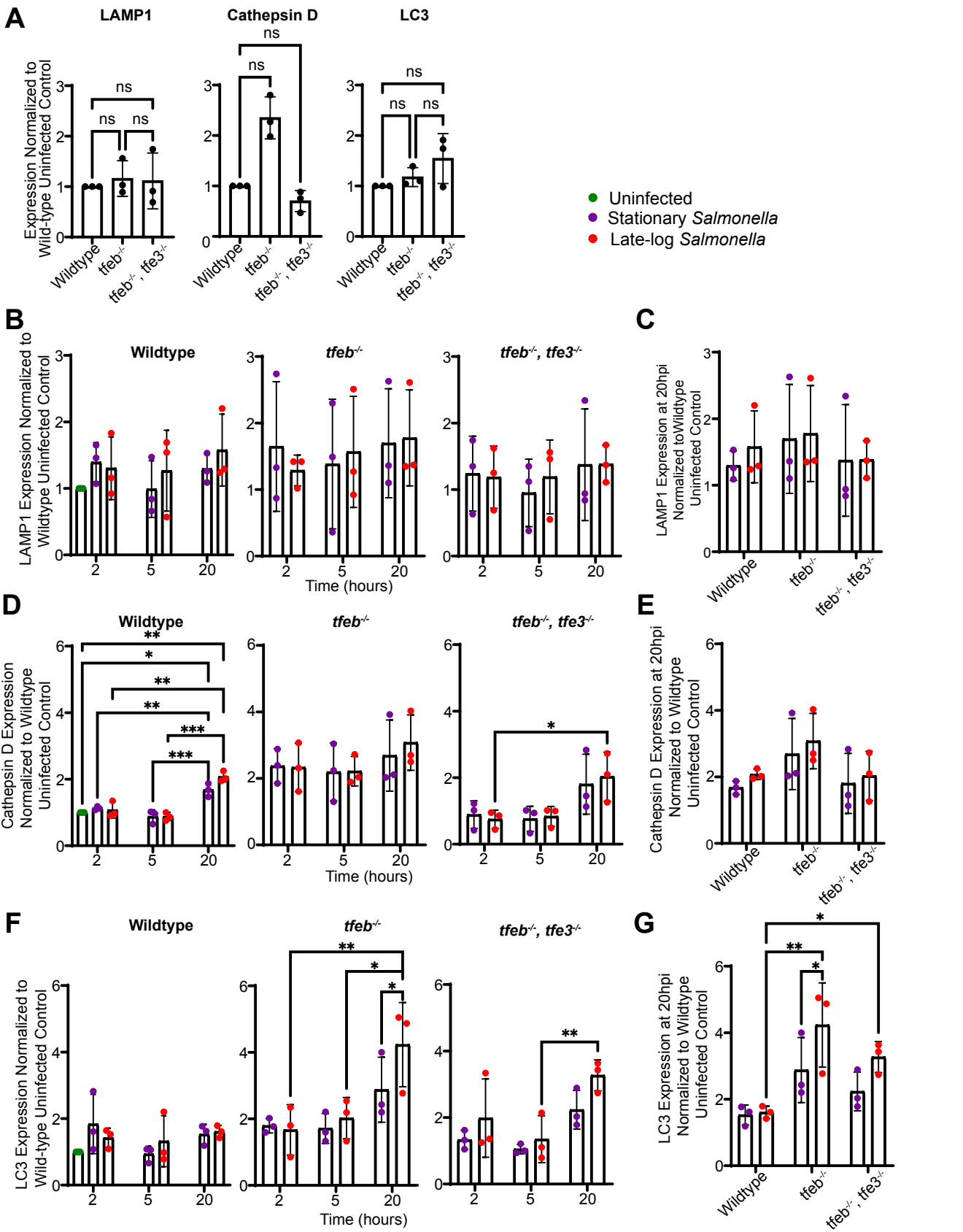
A
LAMP1
Cathepsin D
LC3
Expression Normalized to Wild-type Uninfected Control
ns
Wildtype
tfeb-/-
tfeb-/-, tfe3-/-
Uninfected
Stationary Salmonella
Late-log Salmonella
B
Wildtype
tfeb-/-
tfeb-/-, tfe3-/-
LAMP1 Expression Normalized to Wildtype Uninfected Control
Time (hours)
C
LAMP1 Expression at 20hpi Normalized toWildtype Uninfected Control
D
Cathepsin D Expression Normalized to Wildtype Uninfected Control
E
Cathepsin D Expression at 20hpi Normalized to Wildtype Uninfected Control
F
LC3 Expression Normalized to Wild-type Uninfected Control
G
LC3 Expression at 20hpi Normalized to Wildtype Uninfected Control

Figure 8

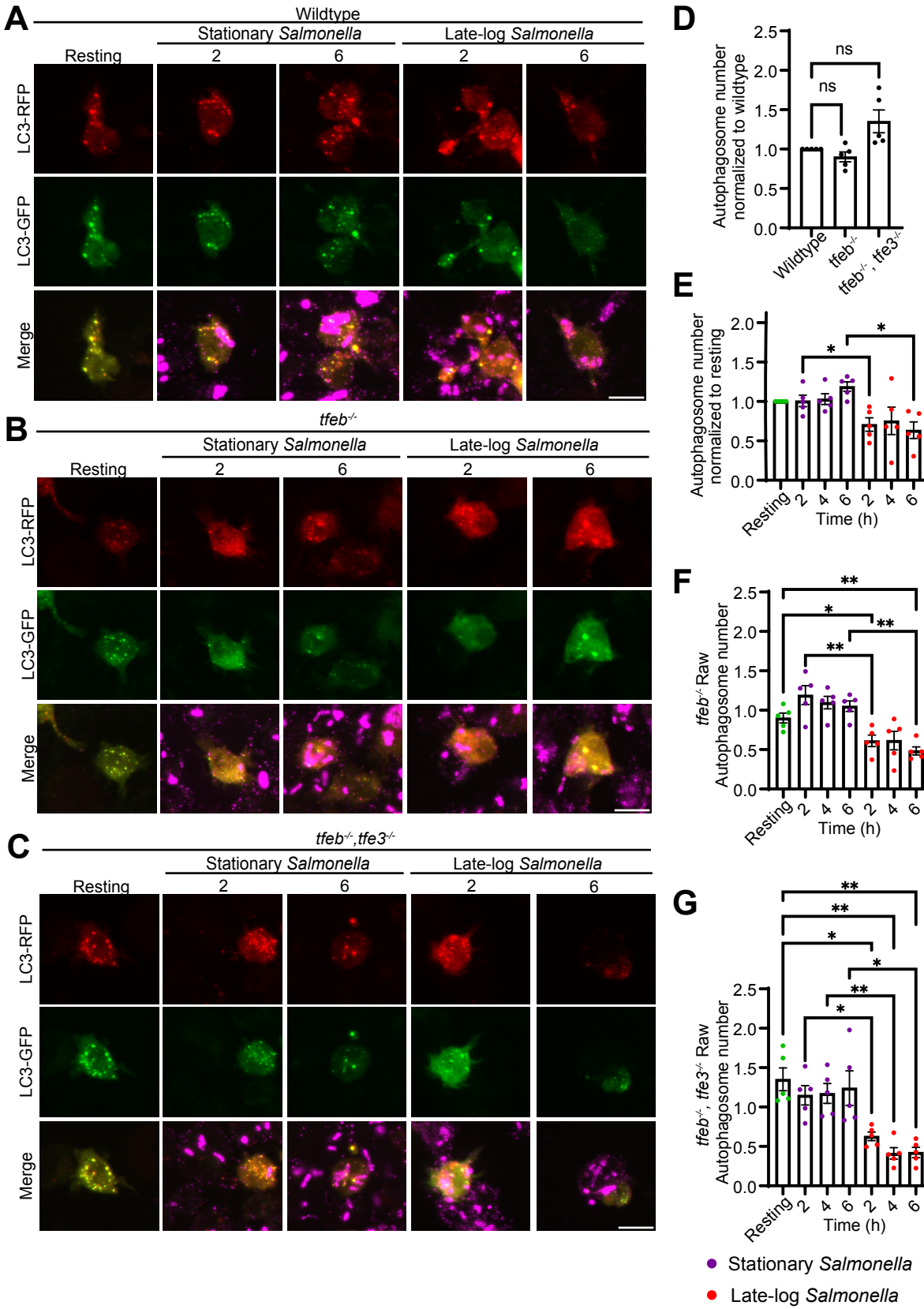
A
Wildtype
Stationary Salmonella
Late-log Salmonella
Resting
2
6
2
6
LC3-RFP
LC3-GFP
Merge
B
tfeb-/-
C
tfeb-/-,tfe3-/-
D
Autophagosome number normalized to wildtype
ns
ns
Wildtype
tfeb-/-
tfeb-/-, tfe3-/-
E
Autophagosome number normalized to resting
Time (h)
F
tfeb-/- Raw Autophagosome number
G
tfeb-/-, tfe3-/- Raw Autophagosome number
Stationary Salmonella
Late-log Salmonella

Figure 9

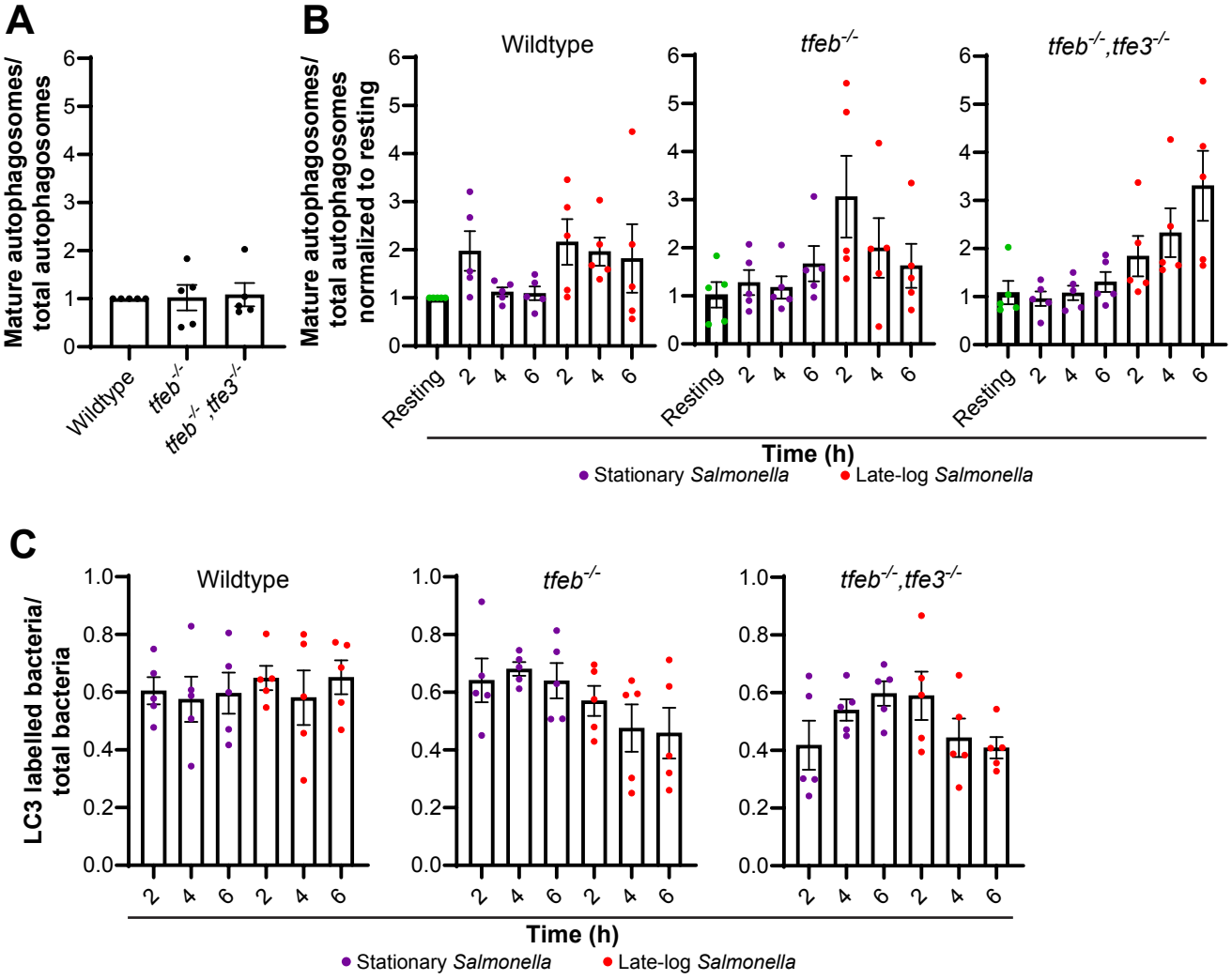
A
Mature autophagosomes/ total autophagosomes
Wildtype
tfeb-/-
tfeb-/-,tfe3-/-
B
Mature autophagosomes/ total autophagosomes normalized to resting
Wildtype
tfeb-/-
tfeb-/-,tfe3-/-
Resting
Time (h)
Stationary Salmonella
Late-log Salmonella
C
LC3 labelled bacteria/ total bacteria
Wildtype
tfeb-/-
tfeb-/-,tfe3-/-
Time (h)
Stationary Salmonella
Late-log Salmonella

Figure 10

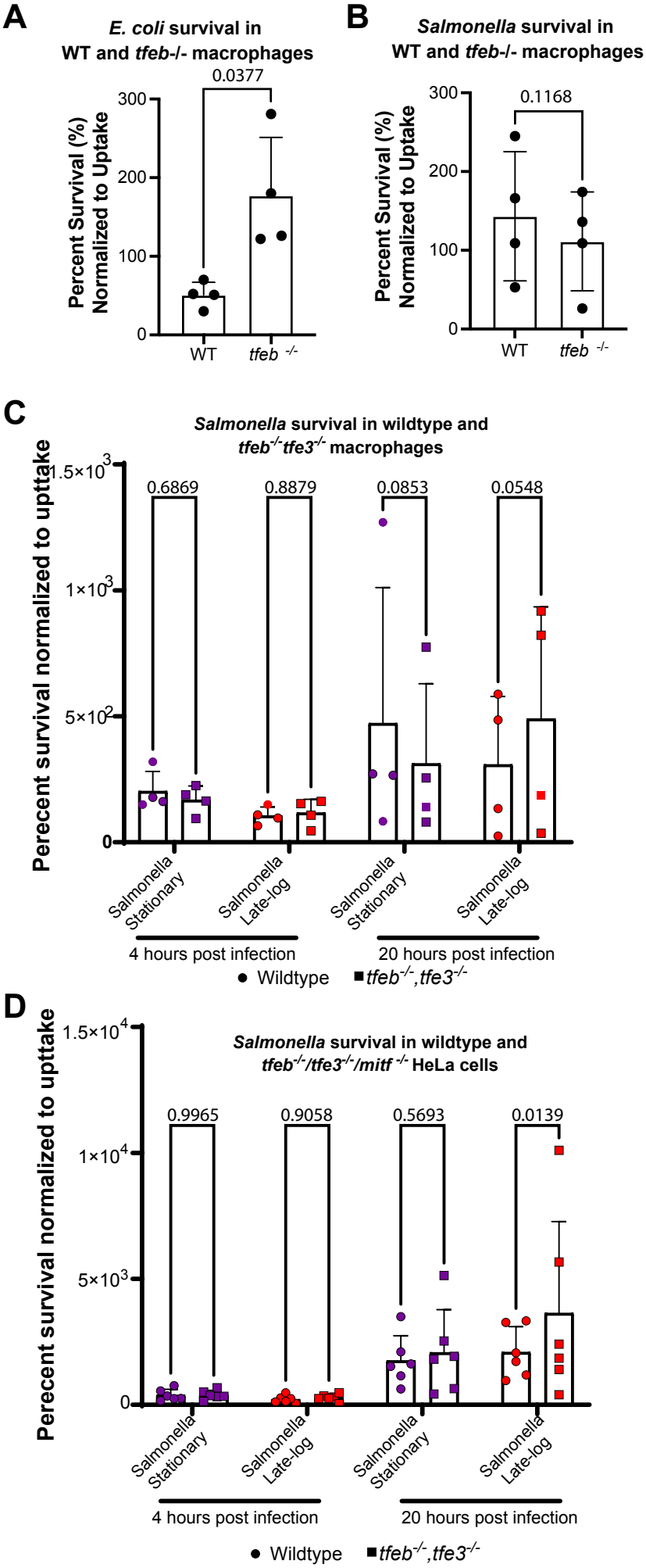
A
E. coli survival in
WT and tfeb-/- macrophages
0.0377
Percent Survival (%)
Normalized to Uptake
300
200
100
0
WT
tfeb -/-
B
Salmonella survival in
WT and tfeb-/- macrophages
0.1168
Percent Survival (%)
Normalized to Uptake
300
200
100
0
WT
tfeb -/-
C
Salmonella survival in wildtype and
tfeb-/-tfe3-/- macrophages
Perecent survival normalized to upttake
1.5×10^3
1×10^3
5×10^2
0
0.6869
0.8879
0.0853
0.0548
Salmonella Stationary
Salmonella Late-log
Salmonella Stationary
Salmonella Late-log
4 hours post infection
20 hours post infection
Wildtype
tfeb-/-,tfe3-/-
D
Salmonella survival in wildtype and
tfeb-/-/tfe3-/-/mitf -/- HeLa cells
Perecent survival normalized to upttake
1.5×10^4
1×10^4
5×10^3
0
0.9965
0.9058
0.5693
0.0139
Salmonella Stationary
Salmonella Late-log
Salmonella Stationary
Salmonella Late-log
4 hours post infection
20 hours post infection
Wildtype
tfeb-/-,tfe3-/-

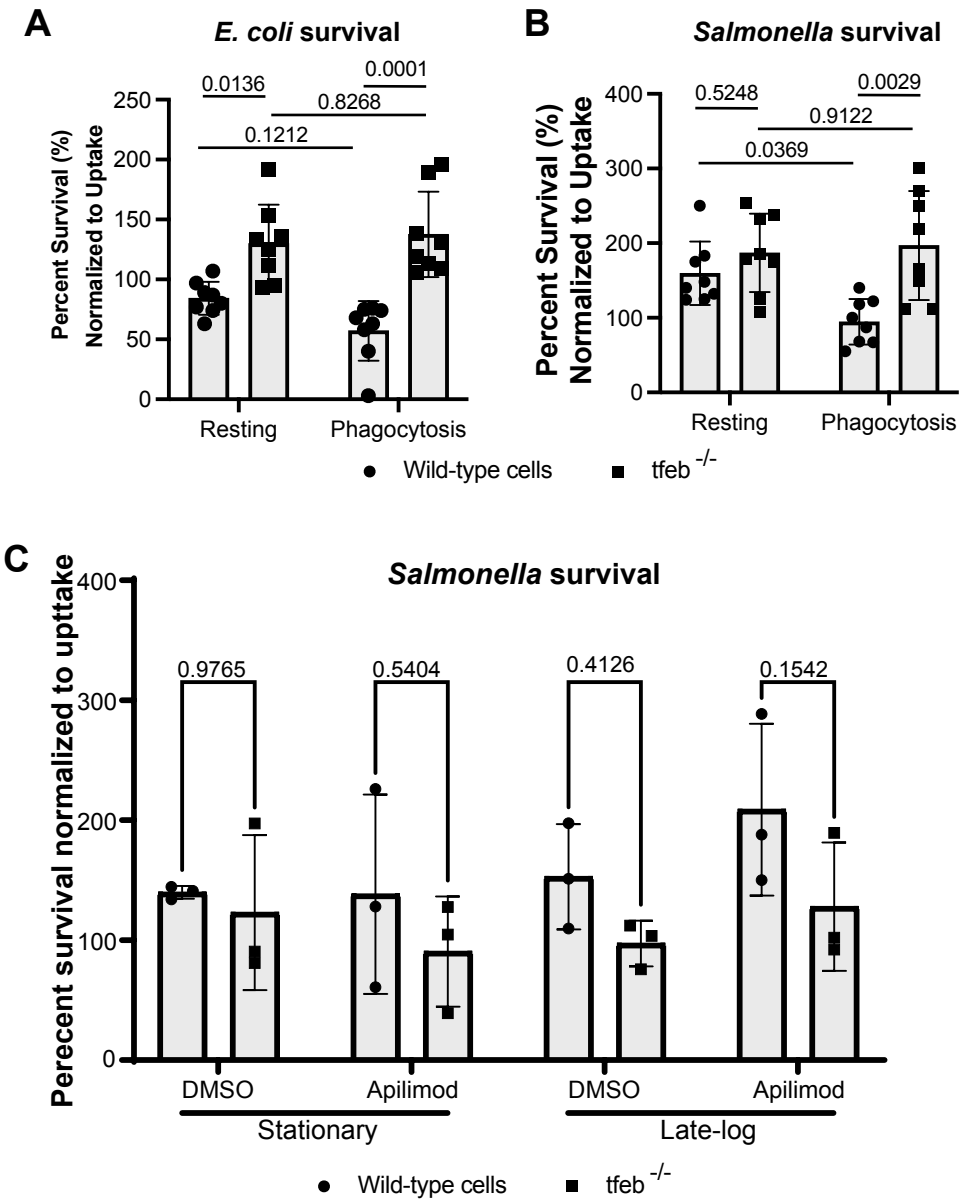
A
E. coli survival
Percent Survival (%)
Normalized to Uptake
0.0136
0.0001
0.8268
0.1212
Resting
Phagocytosis
B
Salmonella survival
Percent Survival (%)
Normalized to Uptake
0.5248
0.0029
0.9122
0.0369
Resting
Phagocytosis
Wild-type cells
tfeb -/-
C
Salmonella survival
Perecent survival normalized to upttake
0.9765
0.5404
0.4126
0.1542
DMSO
Apilimod
DMSO
Apilimod
Stationary
Late-log
Wild-type cells
tfeb -/-

Figure 12